

Supplementary Materials

Sustainable synthesis, antiproliferative and acetylcholinesterase inhibition of 1,4- and 1,2-naphthoquinone derivatives

Rafaela G. Cabral ^{1,2}, Gonçalo Viegas ¹, Rita Pacheco ^{1,2}, Ana Catarina Sousa ^{1,2*} and Maria Paula Robalo ^{1,2*}

¹ Departamento de Engenharia Química, Instituto Superior de Engenharia de Lisboa, Instituto Politécnico de Lisboa, 1959-007 Lisboa, Portugal;

² Centro de Química Estrutural, Institute of Molecular Sciences, Instituto Superior Técnico, Universidade de Lisboa 1049-001 Lisboa, Portugal; ;

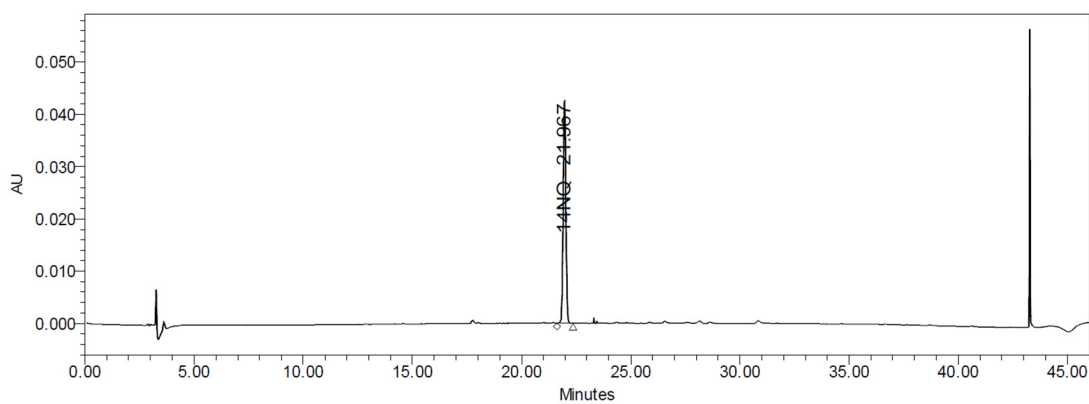
* Correspondence: MPR: mprobalo@deq.isel.ipl.pt and ACS: acsousa@deq.isel.ipl.pt.

Contents

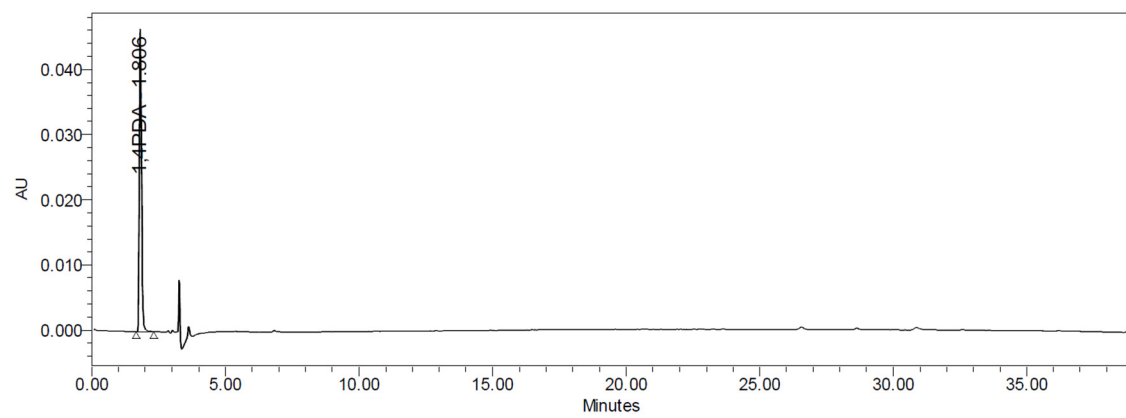
1. HPLC profiles	S2
2. Electrochemical studies	S3
3. <i>In silico</i> analysis	S9
4. <i>In vitro</i> cytotoxicity against human hepatocarcinoma cell line HepG2	S10
5. Inhibition of acetylcholinesterase activity	S12
6. Molecular docking studies	S13
7. 1D and 2D NMR spectra	S14
8. ESI/MS spectra	S31
9. HRESI/TOFMS spectra	S40

1. HPLC profiles

A)



B)



C)

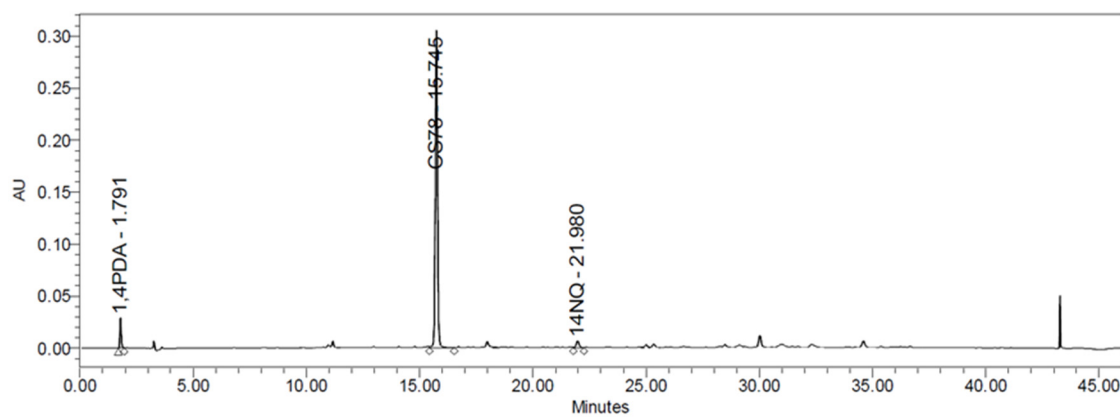


Figure S1. HPLC profiles of **A)** 1,4-NQ; **B)** 1,4-PDA and **C)** MA synthesis of **3a**, at optimized conditions (entry 15. Table 1).

2. Electrochemical studies

Table S1. Electrochemical parameters for 1,4-NQ and derivatives in acetonitrile (potentials are given vs SCE; scan rate: 100 mV.s⁻¹).

Compound	E _{pa} (V)	E _{pc} (V)	E _{1/2} (V)	E _{pa} , E _{pc} (mV)	I _{pa} /I _{pc}
1	-0.62	-0.70	-0.66	80	0.9
	-1.02	-1.36	--	--	--
3a	0.72	0.44	--	--	--
	-0.78	-0.86	-0.82	80	0.9
	-1.27	-1.42	--	--	--
3b	1,04	--	--	--	--
	-0.77	-0.84	-0.81	70	1.0
3c	1,21	--	--	--	--
	-0,79	-0.86	-0.82	70	1.0
	-1,22	-1.34	-1.28	120	1.0
3d	-0.66	-0.74	-0.70	80	1.0
3e	1,55	--	--	--	--
	0.74	--	--	--	--
	-0.74	-0.98	-0.95	70	1.0
	-1.37	-1.47	-1.42	100	1.0
3f	1,40	--	--	--	--
	-0,90	-0.97	-0.94	70	1.0

Table S2. Electrochemical parameters for 1,2-NQ and derivatives in acetonitrile (potentials are given vs SCE; scan rate: 0.100 V.s⁻¹).

Compound	E _{pa} (V)	E _{pc} (V)	E _{1/2} (V)	E _{pa} , E _{pc} (mV)	I _{pa} /I _{pc}
2	-0.44	-0.55	-0.50	110	1.0
	-0.84	-0.98	-0.91	140	1.0
4a	0.81	--	--	--	--
	-0.47	-0.67	--	--	--
4b	1,16	--	--	--	--
	0,93	--	--	--	--
	-0,36	-0.61	--	--	--
4c	1.07	--	--	--	--
	-0.44	-0.67	--	--	--
	-1.30	-1.58	--	--	--
4d	0.76	--	--	--	--
	-0.33	-0.47	--	--	--
	--	-0.84	--	--	--
4g	0.92	--	--	--	--
	0.75	--	--	--	--
	-0.35	-0.63	--	--	--
	--	-1.43	--	--	--
4h	1.39	--	--	--	--
	1.08	--	--	--	--
	--	0.13	--	--	--
	-0.15	-0.57	--	--	--
	--	-0.81	--	--	--
	-0.75	-0.98	--	--	--
4e	1.48	--	--	--	--
	1.01	--	--	--	--
	-0.63	-0.78	-0.71	150	--
4f	1.38	--	--	--	--
	0.91	--	--	--	--
	--	-0.52	--	--	--
	-0.57	-0.69	-0.63	120	0.9

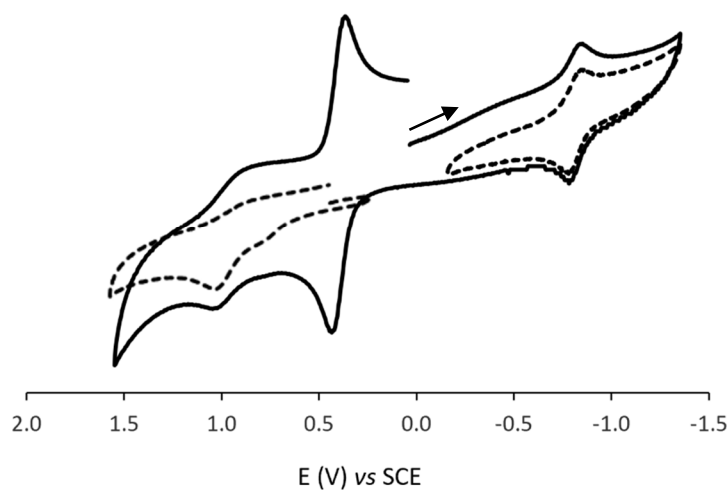


Figure S2. Cyclic voltammogram of **3b** in ACN + TBAPF₆ showing the ferrocene redox pair (black line) and the isolated redox processes (dashed line) at scan rate of 100 mV.s⁻¹.

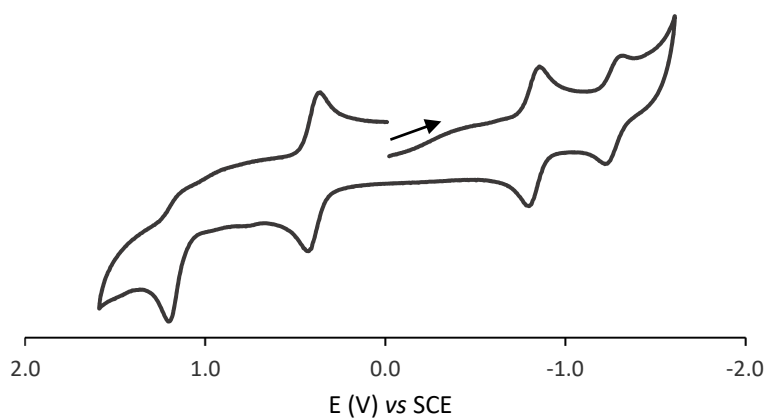


Figure S3. Cyclic voltammogram of **3c** in ACN + TBAPF₆, showing the ferrocene redox pair at scan rate of 100 mV.s⁻¹.

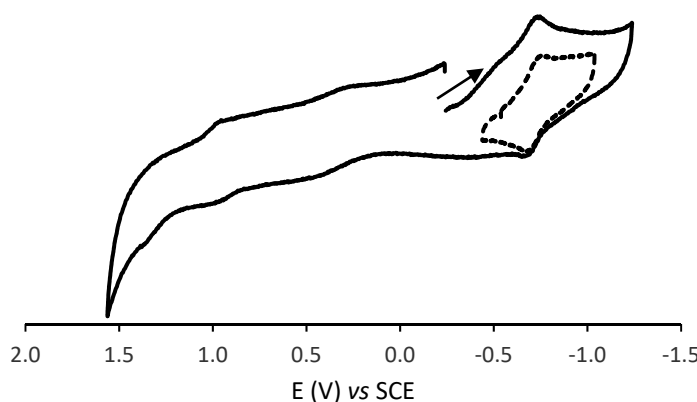


Figure S4. Cyclic voltammogram of **3d** in ACN + TBAPF₆ (black line) showing the isolated redox process (dashed line) at scan rate of 100 mV.s⁻¹.

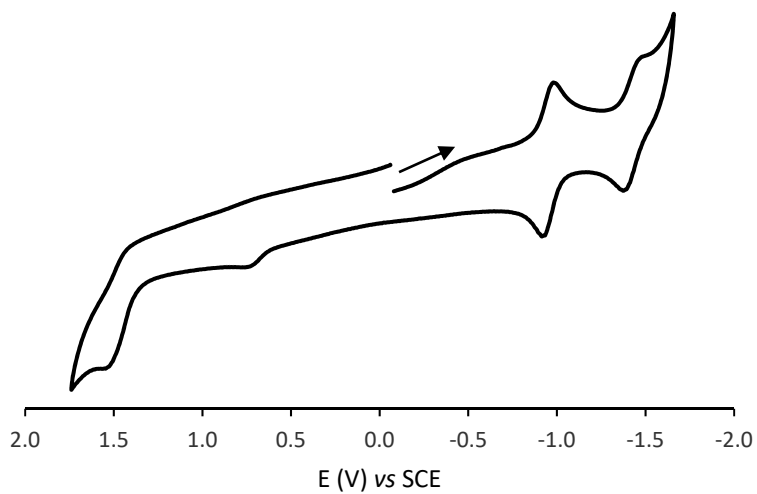


Figure S5. Cyclic voltammogram of **3e** in ACN + TBAPF₆ at scan rate of 100 mV.s⁻¹.

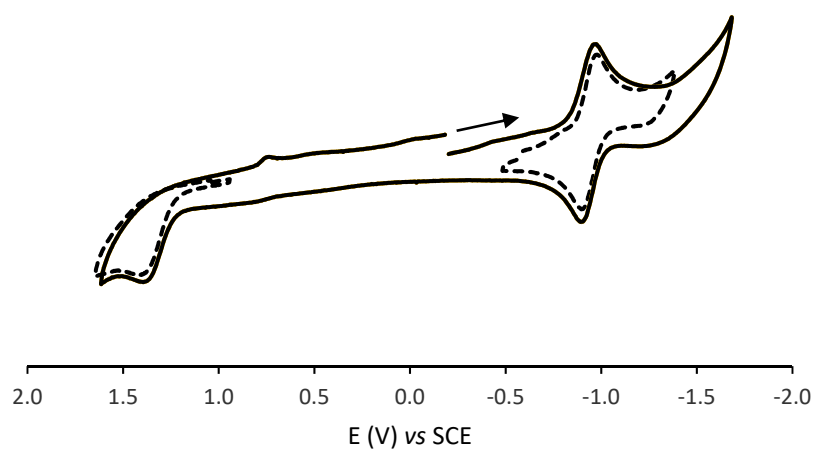


Figure S6. Cyclic voltammogram of **3f** in ACN + TBAPF₆ (black line) showing the isolated redox processes (dashed line) at scan rate of 100 mV.s⁻¹.

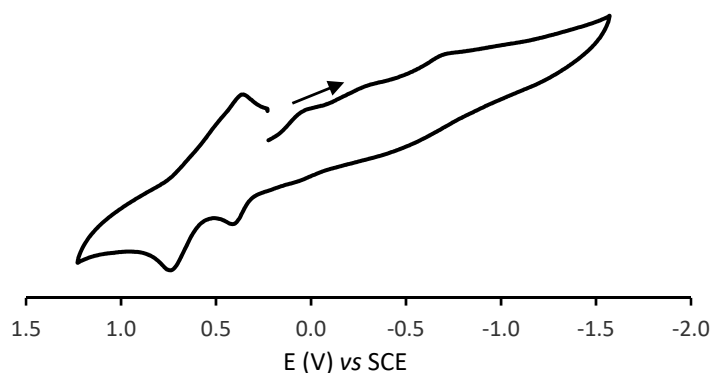


Figure S7. Cyclic voltammogram of **4a** in ACN + TBAPF₆ showing the ferrocene redox pair at scan rate of 100 mV.s⁻¹.

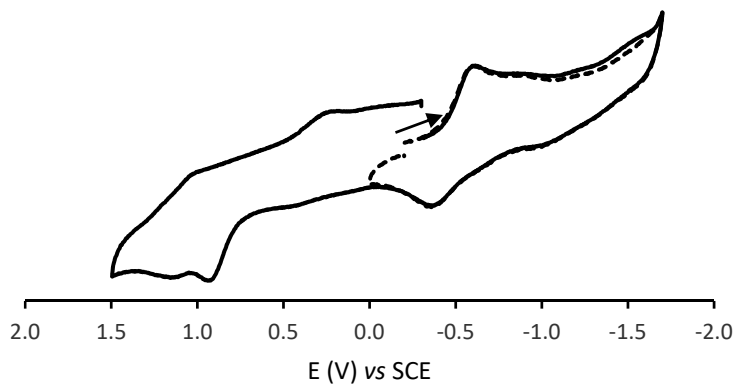


Figure S8. Cyclic voltammogram of **4b** in ACN + TBAPF₆ (black line) showing the isolated redox process (dashed line) at scan rate of 100 mV.s⁻¹.

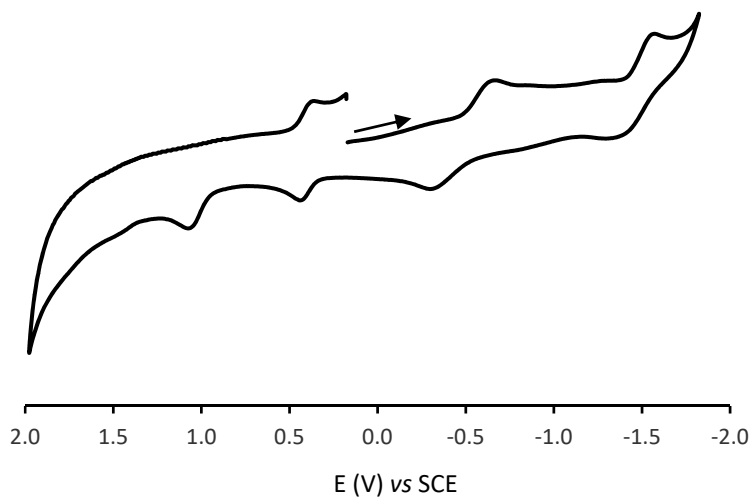


Figure S9. Cyclic voltammogram of **4c** in ACN + TBAPF₆ showing the ferrocene redox pair at scan rate of 100 mV.s⁻¹.

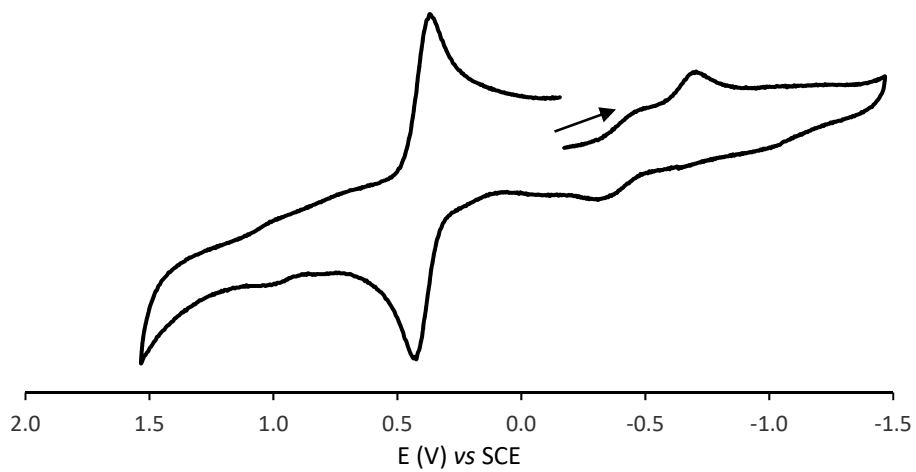


Figure S10. Cyclic voltammogram of **4d** in ACN + TBAPF₆ showing the ferrocene redox pair at scan rate of 100 mV.s⁻¹.

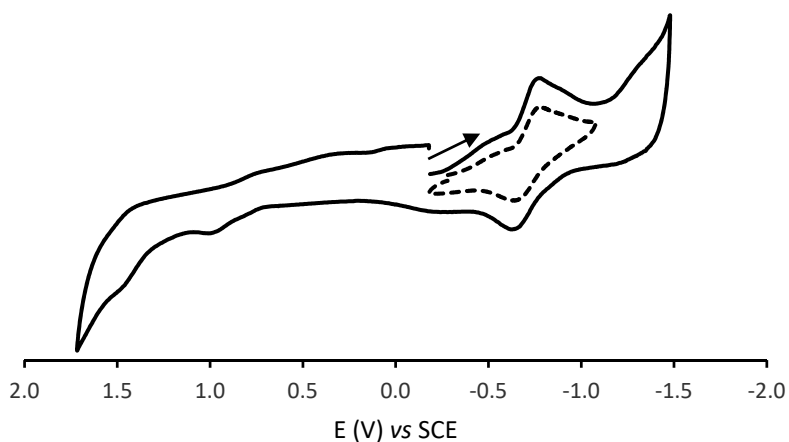


Figure S11. Cyclic voltammogram of **4e** in ACN + TBAPF₆ (black line) showing the isolated redox process (dashed line) at scan rate of 100 mV.s⁻¹.

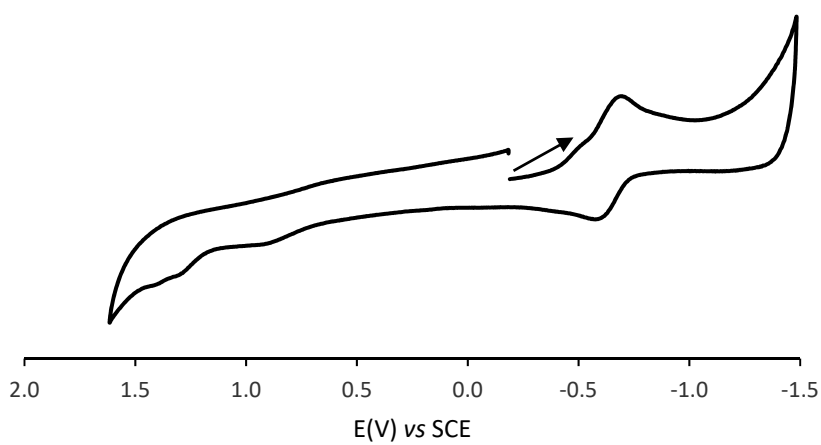


Figure S12. Cyclic voltammogram of **4f** in ACN + TBAPF₆ at scan rate of 100 mV.s⁻¹.

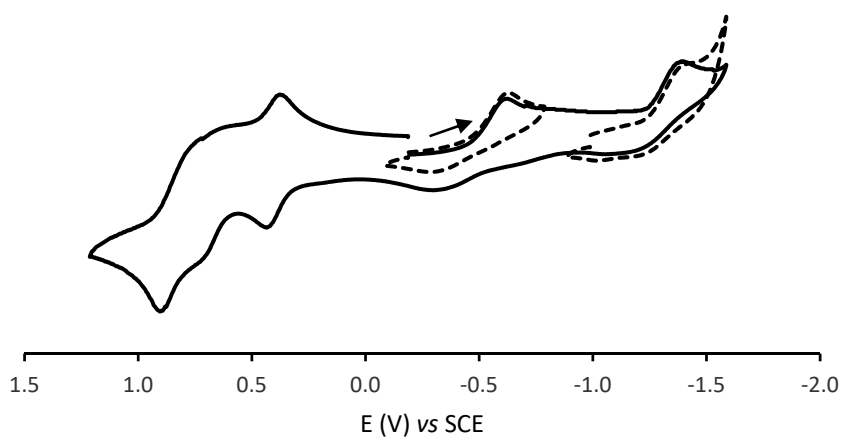


Figure S13. Cyclic voltammogram of **4g** in ACN + TBAPF₆ showing the ferrocene redox pair (black line) and the isolated redox processes (dashed line) at scan rate of 100 mV.s⁻¹.

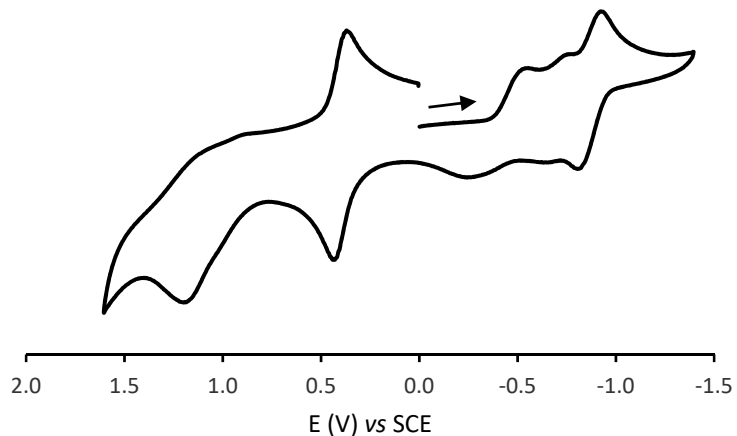


Figure S14. Cyclic voltammogram of **4h** in ACN + TBAPF₆ showing the ferrocene redox pair (black line) and the isolated redox processes (dashed line) at scan rate of 100 mV.s⁻¹.

3. In silico analysis

Table S3. Lipinski's parameters for compounds **1** and **3a-f** estimated using Molinspiration.

Compound	Lipinski's parameters						ABS% ¹	
	M (g/mol)	mi LogP	TPSA	n _{OH}	n _{OHNH}	n _{rot}		
1	158.16	1.67	34.14	2	0	0	0	98.83
3a	264.28	2.66	72.19	4	3	2	0	84.55
3b	265.27	3.11	66.4	4	2	2	0	92.53
3c	279.3	3.64	55.4	4	1	3	0	97.78
3d	274.28	3.34	69.96	4	1	2	0	97.60
3e	229.28	2.89	46.17	3	1	4	0	97.42
3f	229.28	2.45	37.38	3	0	3	0	99.37

Table S4. Lipinski's parameters for compounds **2** and **4a-h** estimated using Molinspiration.

Compound	Lipinski's parameters						ABS% ¹	
	M (g/mol)	mi LogP	TPSA	n _{OH}	n _{OHNH}	n _{rot}		
2	158.16	1.67	34.14	2	0	0	0	98.83
4a	264.28	2.66	72.19	4	3	2	0	84.55
4b	265.27	3.11	66.4	4	2	2	0	92.53
4c	279.30	3.64	55.4	4	1	3	0	97.78
4d	274.28	3.34	69.96	4	1	2	0	97.60
4g	340.38	5.58	91.99	4	2	2	0	97.18
4h	265.27	3.32	66.4	4	2	2	0	92.53
4e	229.28	2.89	46.17	3	1	4	0	97.42
4f	229.28	2.45	37.38	3	0	3	0	99.37

$$\text{ABS\%} = 100 \times [\exp(-10^{0.506 - 0.0754 \times n_{OH} - 0.141 \times n_{OHNH} + 0.00184 \times MM})]$$

Table S5. Bioactivity scores compounds **1**, **2**, **3a-f** and **4a-h** estimated using Molinspiration.

Compound	GPCR ligand	Ion channel modulator	Kinase inhibitor	Nuclear receptor ligand	Protease inhibitor	Enzyme inhibitor
1	-0.94	-0.46	-0.77	-1	-1.1	-0.34
3a	-0.11	-0.25	0.46	-0.6	-0.3	0.20
3b	-0.12	-0.28	0.40	-0.12	-0.4	-0.14
3c	-0.19	-0.41	0.32	-0.26	-0.42	0.02
3d	-0.11	-0.32	0.47	-0.13	-0.33	0.12
3e	-0.17	-0.32	-0.02	-0.37	-0.42	0.23
3f	-0.19	-0.36	-0.06	-0.46	-0.62	0.04
2	-0.87	-0.4	-0.76	-1.18	-0.91	-0.05
4a	0.01	0.01	0.46	-0.34	-0.06	0.43
4b	-0.01	-0.02	0.39	-0.11	-0.16	0.37
4c	-0.07	-0.16	0.31	-0.24	-0.20	0.24
4d	0.00	-0.07	0.47	-0.12	-0.10	0.34
4g	0.03	-0.05	0.33	-0.13	-0.01	0.24
4h	0.00	-0.32	0.32	-0.32	-0.25	0.32
4e	-0.12	-0.01	-0.01	-0.47	-0.23	0.34
4f	-0.16	-0.14	-0.08	-0.45	-0.38	0.20

A molecule having bioactivity score more than 0.00 is most likely to exhibit considerable biological activities, while values -0.50 to 0.00 are expected to be moderately active and if score is less than -0.50 it is presumed to be inactive.

4. In vitro cytotoxicity against human hepatocarcinoma cell line HepG2

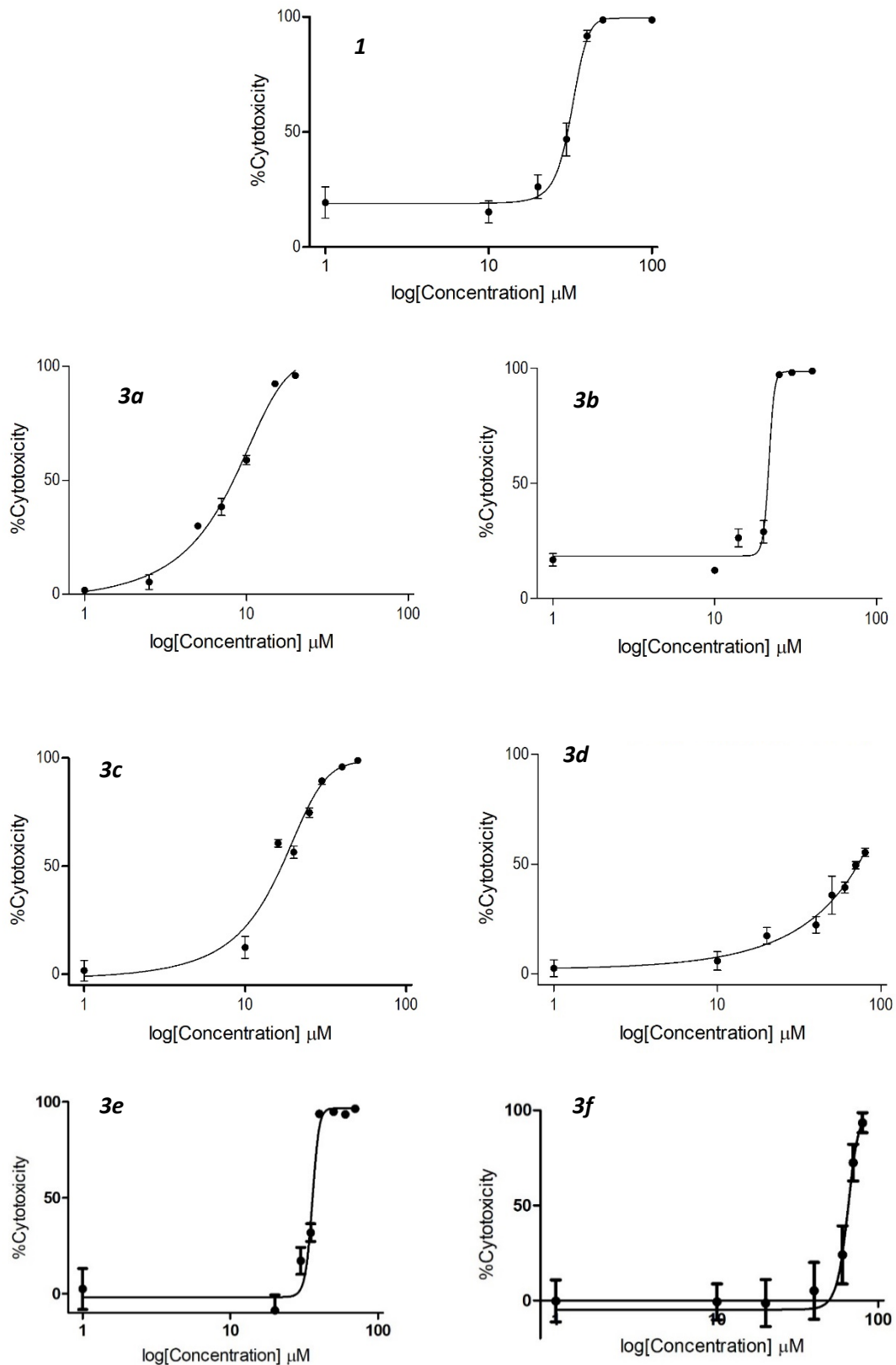


Figure S15. Cytotoxicity profiles of compounds **1** and **3a-f** in HepG2 human cell line.

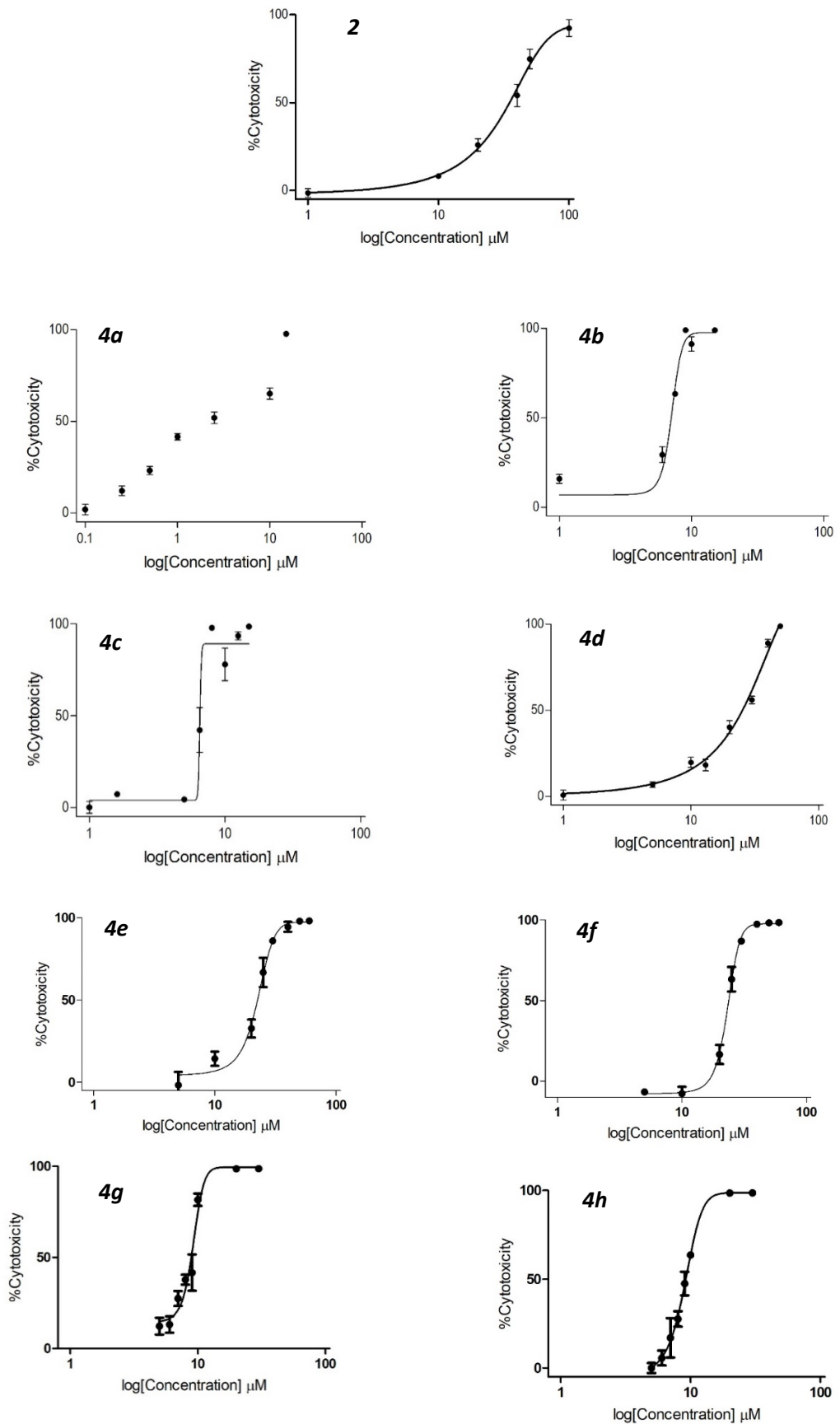


Figure S16. Cytotoxicity profiles of compound **2** and **4a-h** in HepG2 human cell line.

Table S6. The EC₅₀ values for the cytotoxicity of compounds **1**, **2**, **3a-f**, **4a-h** and reference inhibitor doxorubicin against HepG2 cell line.

Compound	EC ₅₀ ($\mu\text{M} \pm \text{SD}$)
1	32.2 \pm 1.4
3a	8.7 \pm 1.3
3b	21.4 \pm 3.9
3c	13.0 \pm 1.8
3d	79.4 \pm 1.4
3e	35.8 \pm 1.5
3f	64.7 \pm 1.4
2	25.6 \pm 1.1
4a	2.7 \pm 1.0
4b	7.1 \pm 1.8
4c	6.5 \pm 1.4
4d	26.8 \pm 1.1
4g	9.2 \pm 2.3
4h	9.1 \pm 3.3
4e	26.8 \pm 1.1
4f	23.1 \pm 1.7
Doxorubicin	1.42 \pm 1.0

All EC₅₀ values are expressed as the mean \pm SD of triplicate determinations.

5. Inhibition of acetylcholinesterase activity

Table S7. AChE Inhibititon_{50 μM} values for compounds **1**, **2**, **3a-f**, **4a-h**.

Compound	Inhibititon _{50μM} ($\mu\text{M} \pm \text{SD}$)
1	50.7 \pm 2.3
3a	23.4 \pm 2.5
3b	16.4 \pm 2.0
3c	25.9 \pm 3.0
3d	25.8 \pm 3.0
3e	48.3 \pm 1.6
3f	47.9 \pm 2.5
2	34.9 \pm 5.2
4a	51.7 \pm 2.1
4b	74.1 \pm 1.1
4c	45.8 \pm 2.9
4d	41.6 \pm 2.4
4g	75.3 \pm 1.3
4h	85.3 \pm 1.3
4e	62.4 \pm 1.5
4f	54.71 \pm 2.0

All Inhibititon_{50 μM} values are expressed as the mean \pm SD of triplicate determinations.

6. Molecular docking studies

Table S8. Molecular docking results of **3b**.

AA	Atom	Interaction type	Distance (Å)
Phe 295	O=C (Quinone ring)	N-H···O(O=C) ^a	2,14
Val 294	O=C (Quinone ring)	C-H···O(O=C)	2,70
Trp 286	C=C (Ar NQ ring)	π-π stacking	5,09
Trp 286	Ar (NQ ring)	π-π stacking	3,90
Trp 286	Ar (Quinone ring)	π-π stacking	5,41
Tyr 341	Ar (Quinone ring)	π-π stacking	4,60
Tyr 341	Ar (NQ ring)	π-π stacking	3,93

^a Conventional Hydrogen Bond

Table S9. Molecular docking results of **4b**.

AA	Atom	Interaction type	Distance (Å)
Gly 120	O-C (Ar ring)	N-H···O(O-C)	2,69
Tyr 124	O=C (Quinone ring)	O-H···O(O=C)	2,69
Tyr 133	O-C (Ar ring)	O-H···O(O-C)	2,35
Glu 202	H-O (Ar ring)	O···H-O(O-C)	1,89
Trp 86	Ar ring	π-π stacking	4,61
Trp 86	Ar ring	π-π stacking	3,76
Tyr 337	Ar (NQ ring)	π-π stacking	4,06
Tyr 337	Ar (Quinone ring)	π-π stacking	5,36
Tyr 341	Ar (NQ ring)	π-π stacking	4,83
Tyr 341	Ar (Quinone ring)	π-π stacking	5,55

^a Conventional Hydrogen Bond

Table S10. Molecular docking results of **4h**.

AA	Atom	Interaction type	Distance (Å)
Tyr 133	O=C (Quinone ring)	O-H···O(O=C)	3,46
Gly 126	O=C (Quinone ring)	O-H···O(O=C)	4,70
Tyr 337	H-N (Ar ring)	O···H-N	3,09
Tyr 341	H-O (Ar ring)	O···H-O(O-C)	3,26
Tyr 341	Ar ring	π-π stacking	4,25
Tyr 337	Ar ring	π-π stacking	4,69
Trp 86	Ar (NQ ring)	π-π stacking	4,15
Trp 86	Ar (Quinone ring)	π-π stacking	4,24

^a Conventional Hydrogen Bond

7. 1D and 2D NMR spectra

Compound **3a**:

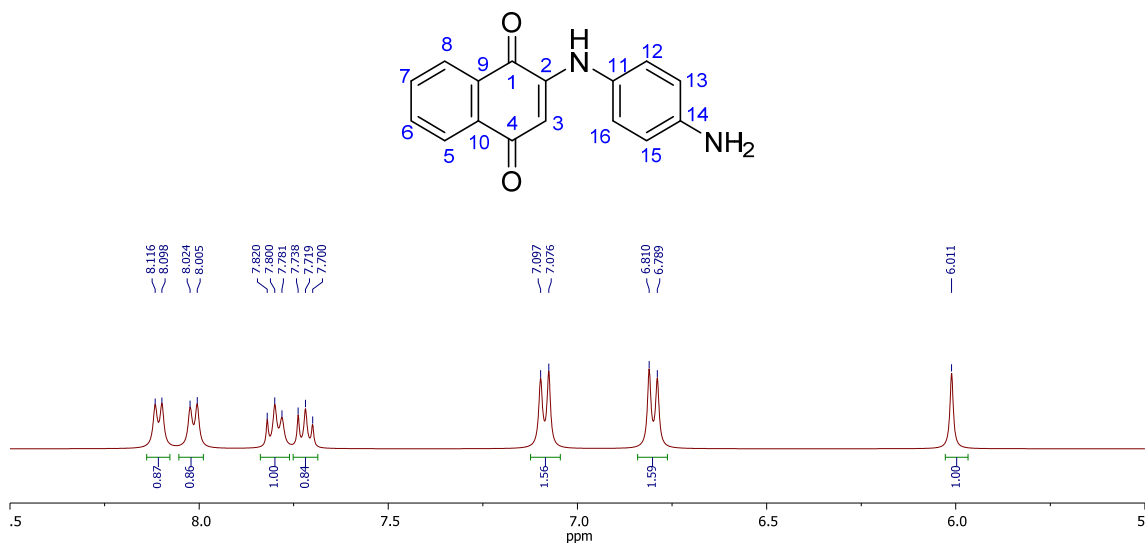


Figure S17. ¹H-NMR spectrum of compound **3a** in MeOD-d₄

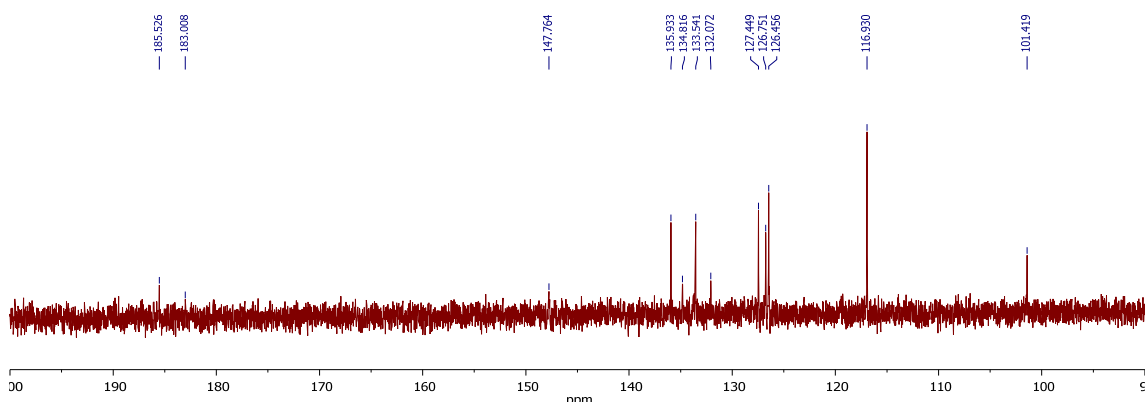


Figure S18. ¹³C-NMR spectrum of compound **3a** in MeOD-d₄

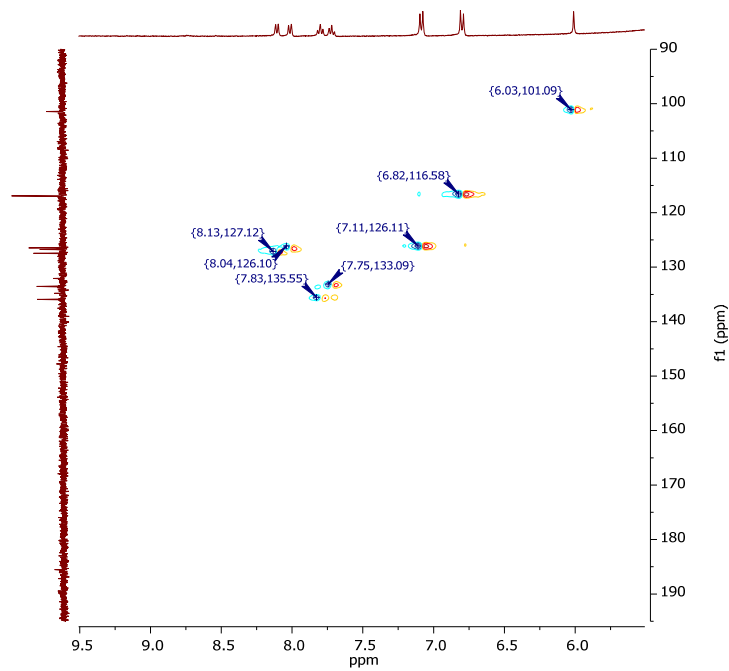


Figure S19. HSQC-NMR spectrum of compound **3a** in $\text{MeOD}-d_4$

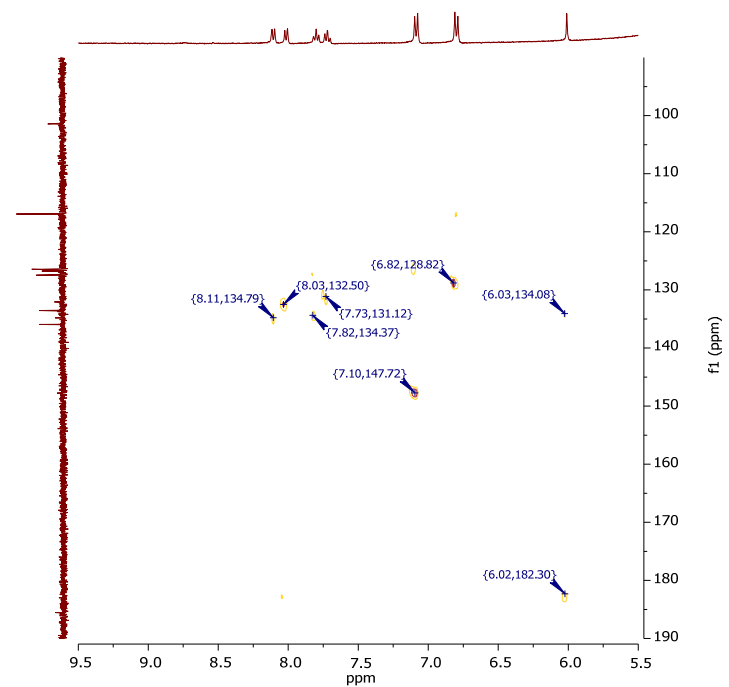


Figure S20. HMBC-NMR spectrum of compound **3a** in $\text{MeOD}-d_4$

Compound 3b:

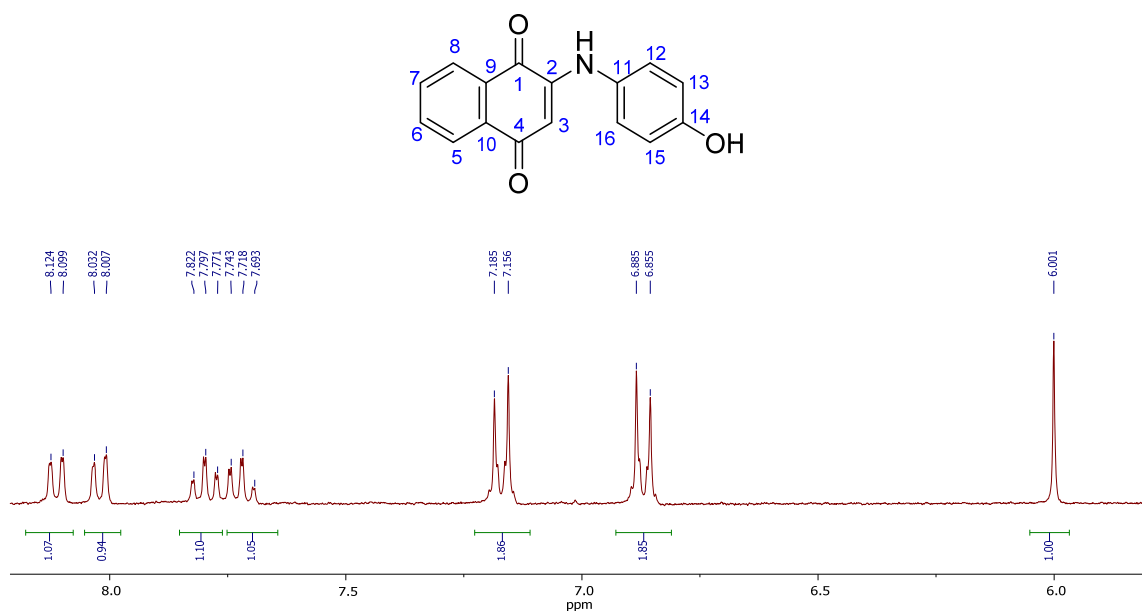


Figure S21. ¹H-NMR spectrum of compound 3b in MeOD-d₄

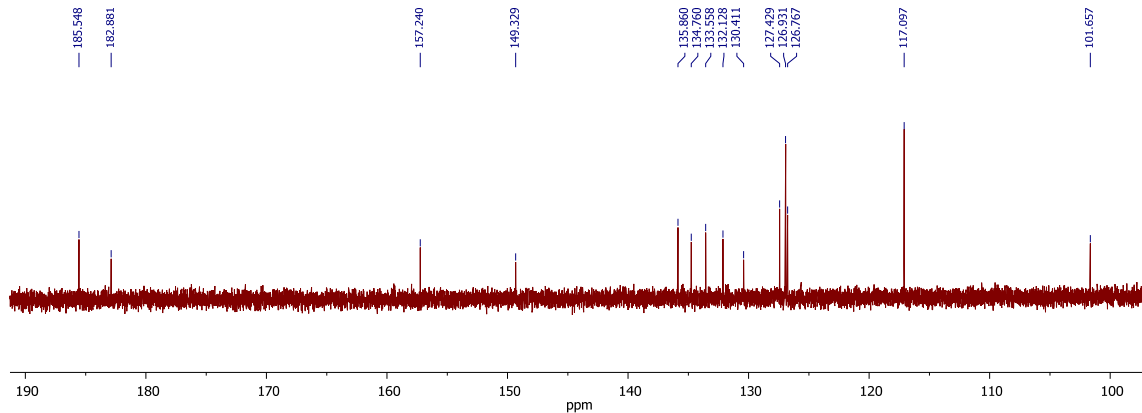


Figure S22. ¹³C-NMR spectrum of compound 3b in MeOD-d₄

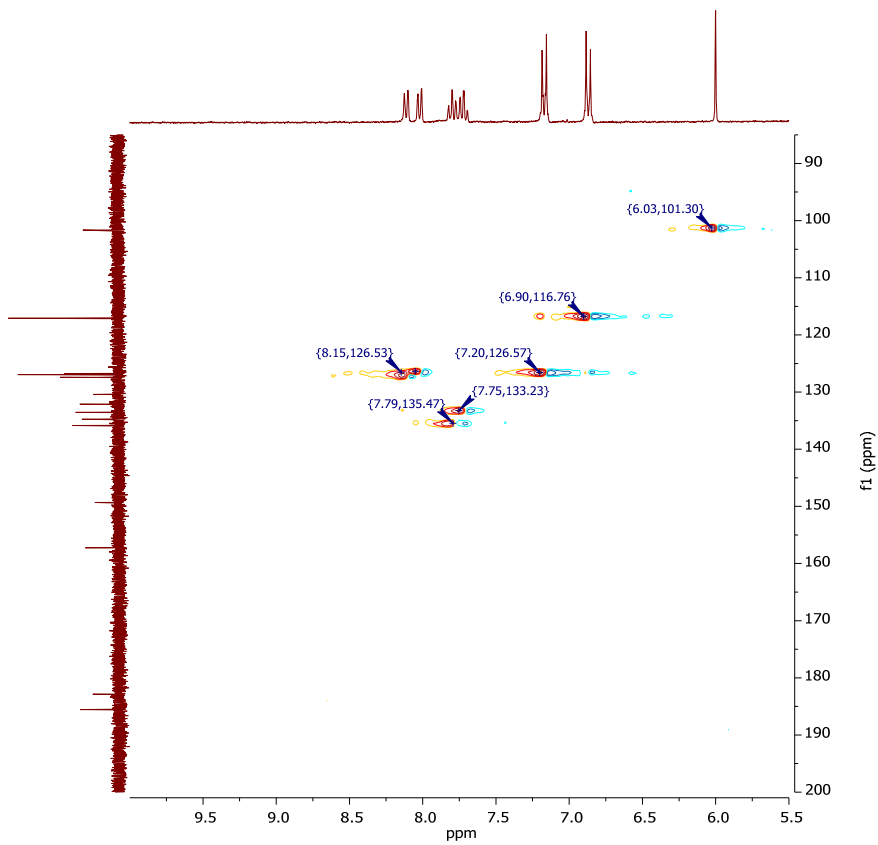


Figure S23. HSQC-NMR spectrum of compound **3b** in $\text{MeOD}-d_4$

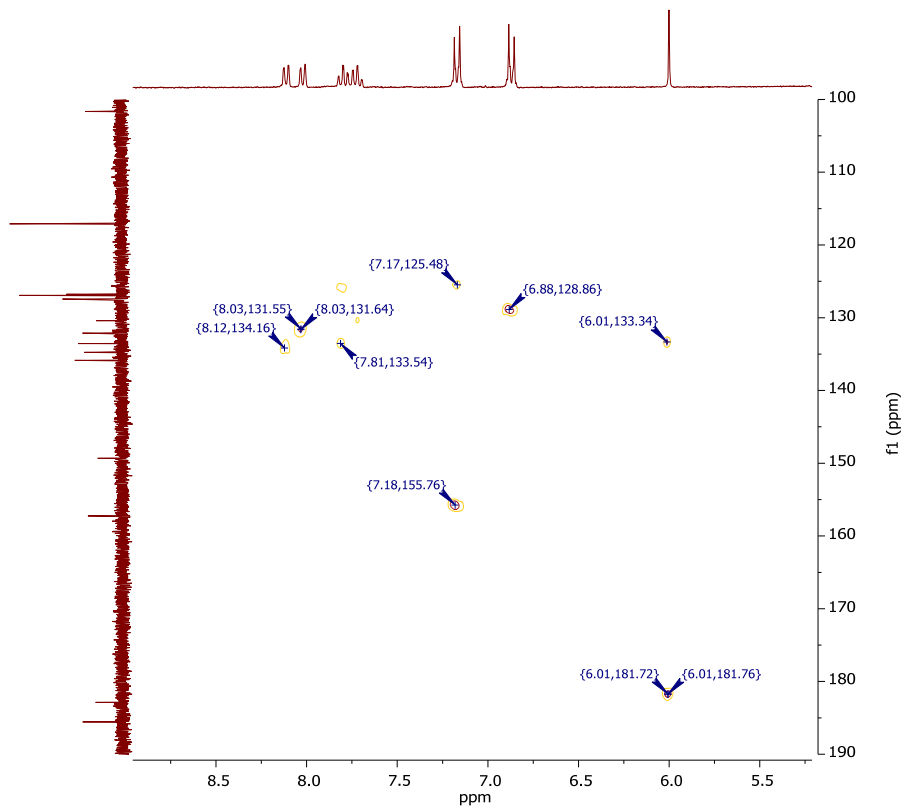


Figure S24. HMBC-NMR spectrum of compound **3b** in $\text{MeOD}-d_4$

Compound 3c:

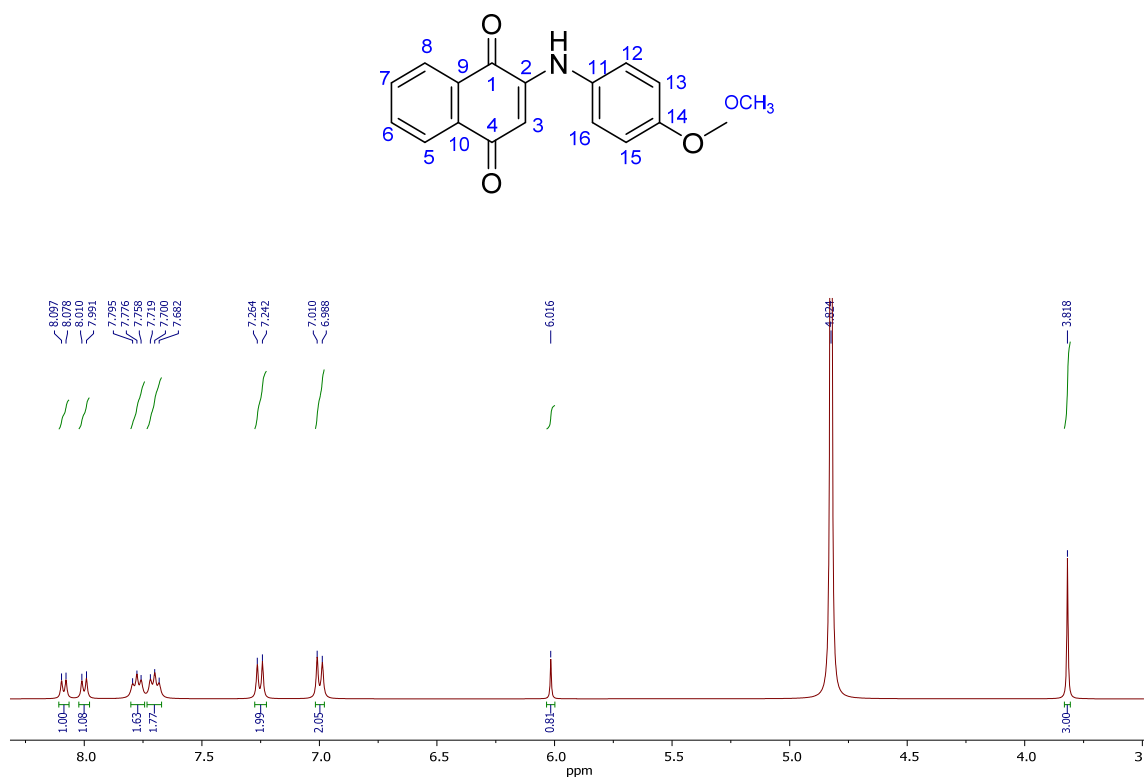


Figure S25. ¹H-NMR spectrum of compound 3c in MeOD-*d*₄

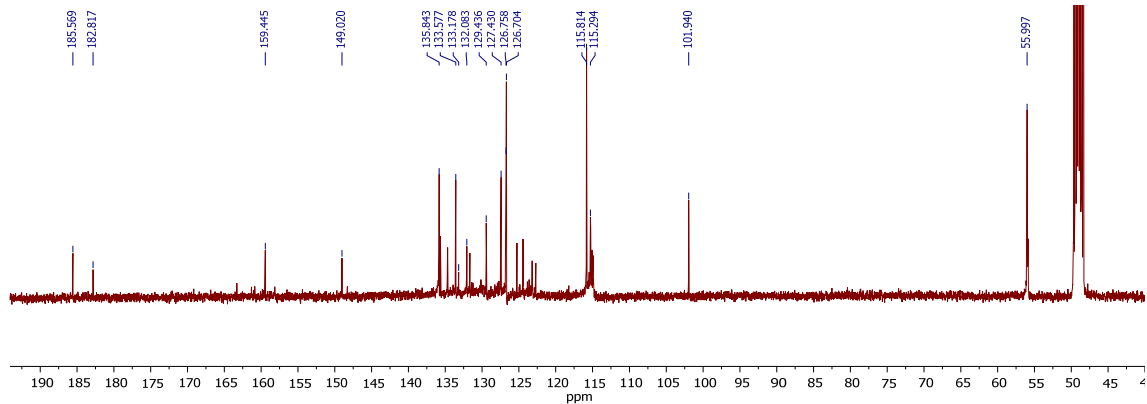


Figure S26. ¹³C-NMR spectrum of compound 3c in MeOD-*d*₄

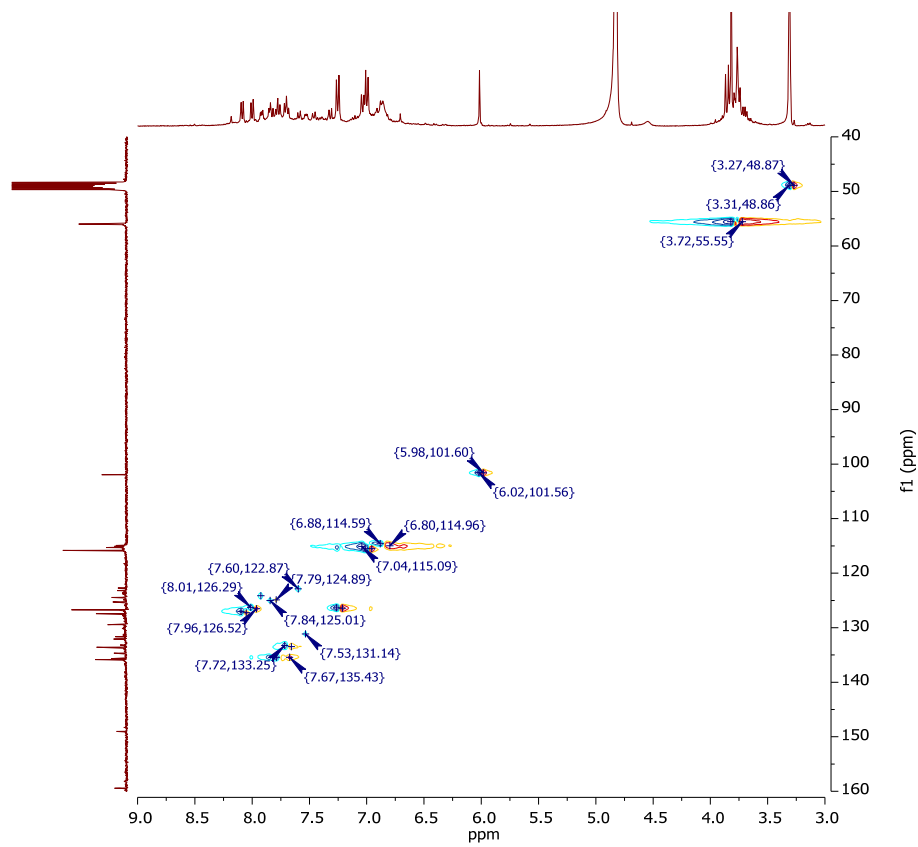


Figure S27. HSQC-NMR spectrum of compound **3c** in $\text{MeOD}-d_4$

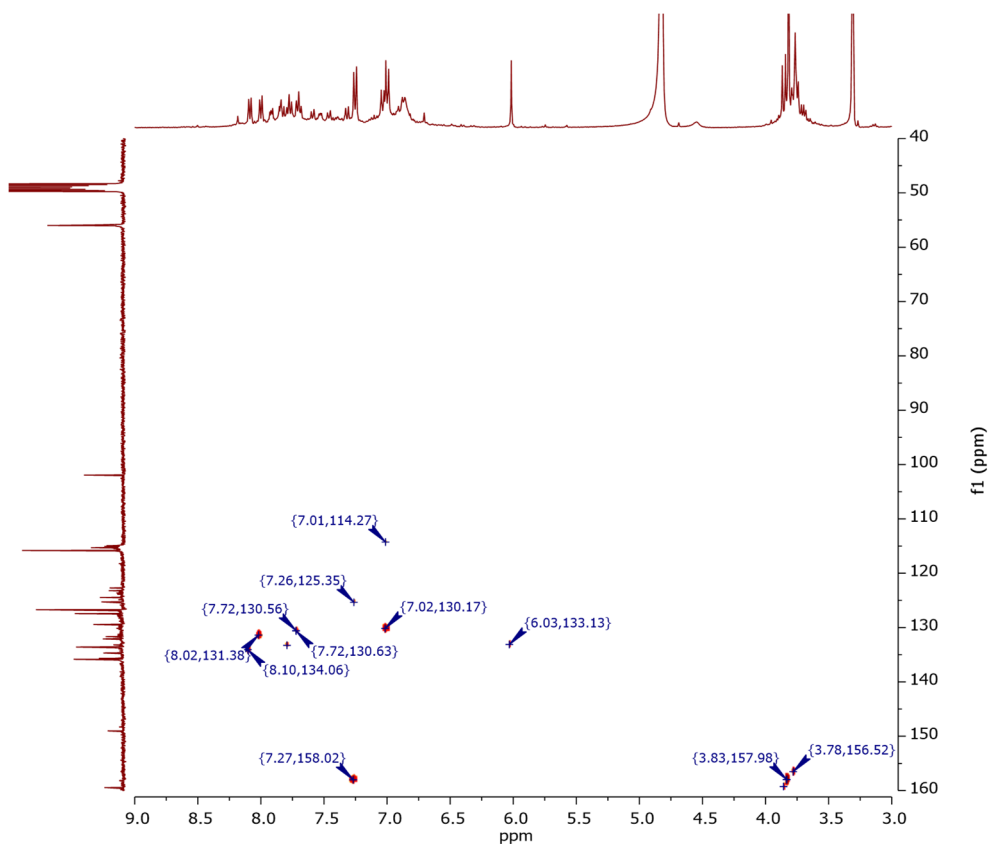


Figure S28. HMBC-NMR spectrum of compound **3c** in $\text{MeOD}-d_4$

Compound 3d:

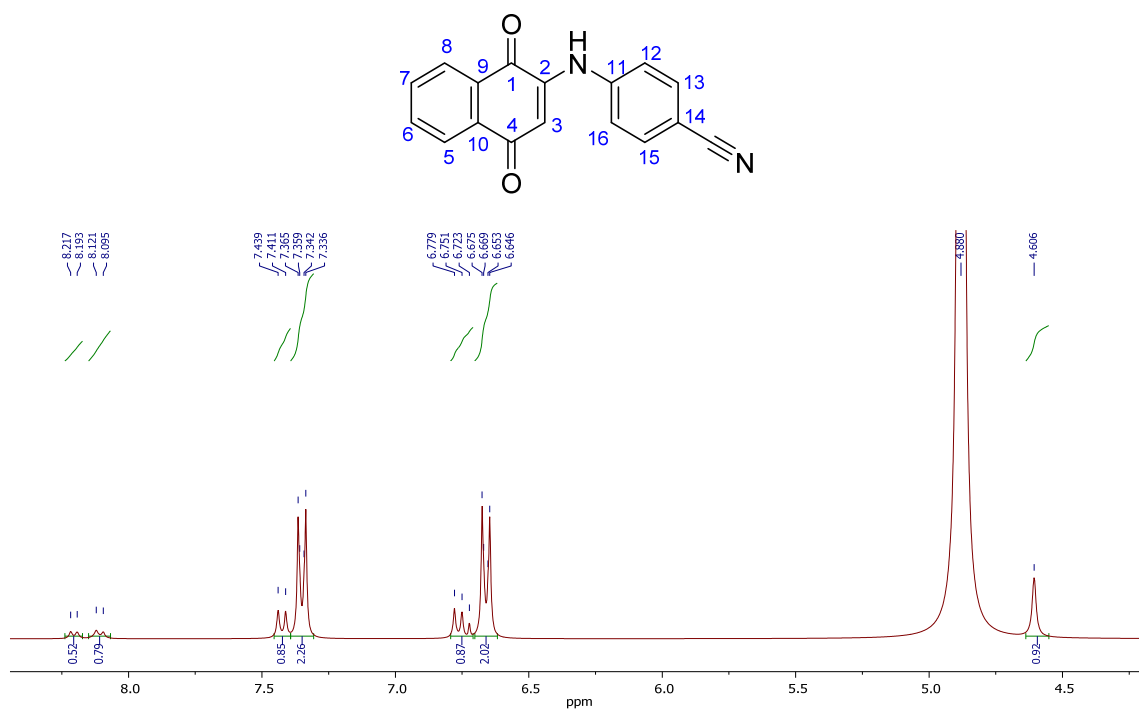


Figure S29. ¹H-NMR spectrum of compound **3d** in MeOD-d₄

Compound 3e:

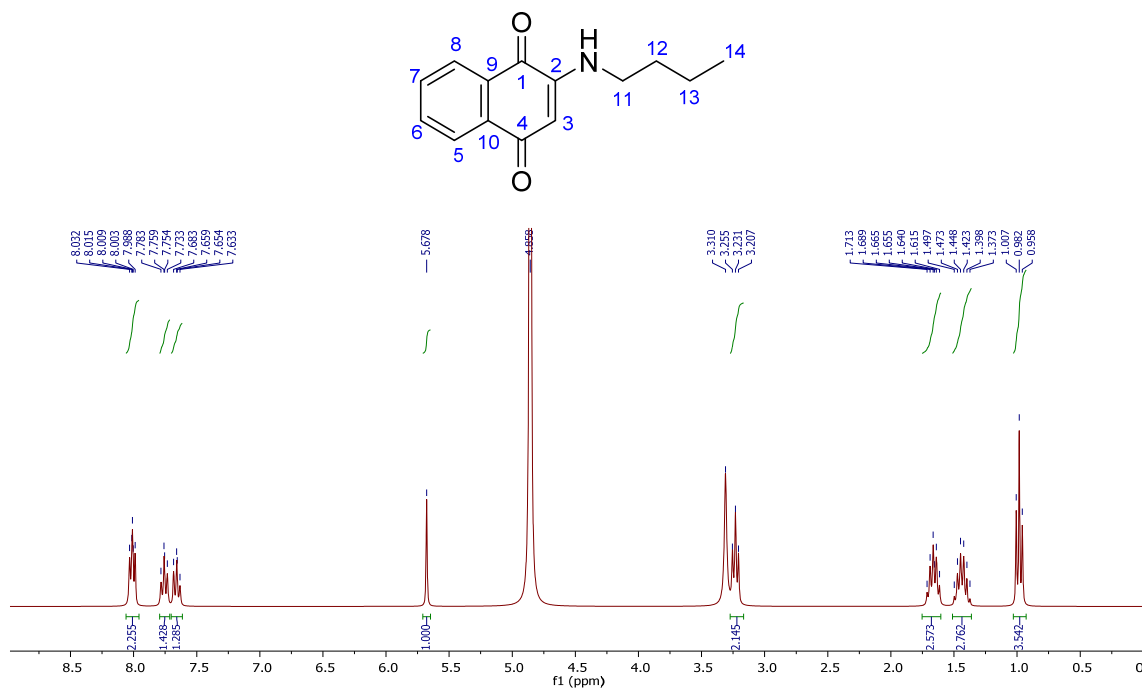


Figure S30. ^1H -NMR spectrum of compound 3e in $\text{MeOD}-d_4$

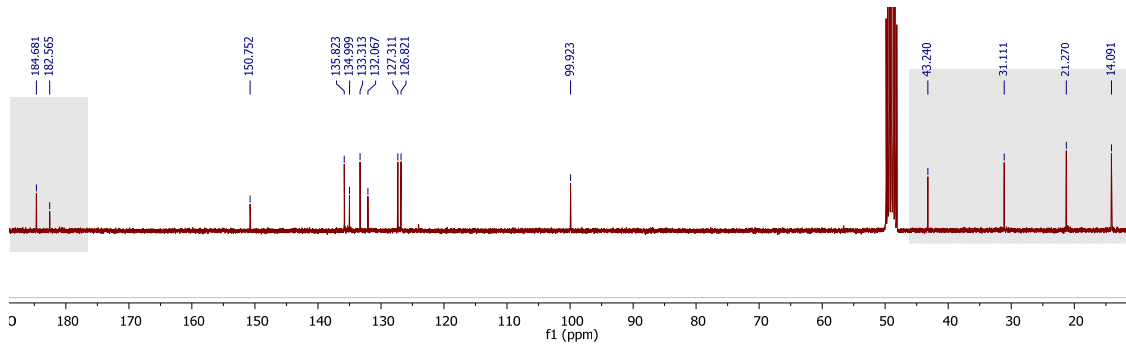


Figure S31. ^{13}C -NMR spectrum of compound 3e in $\text{MeOD}-d_4$

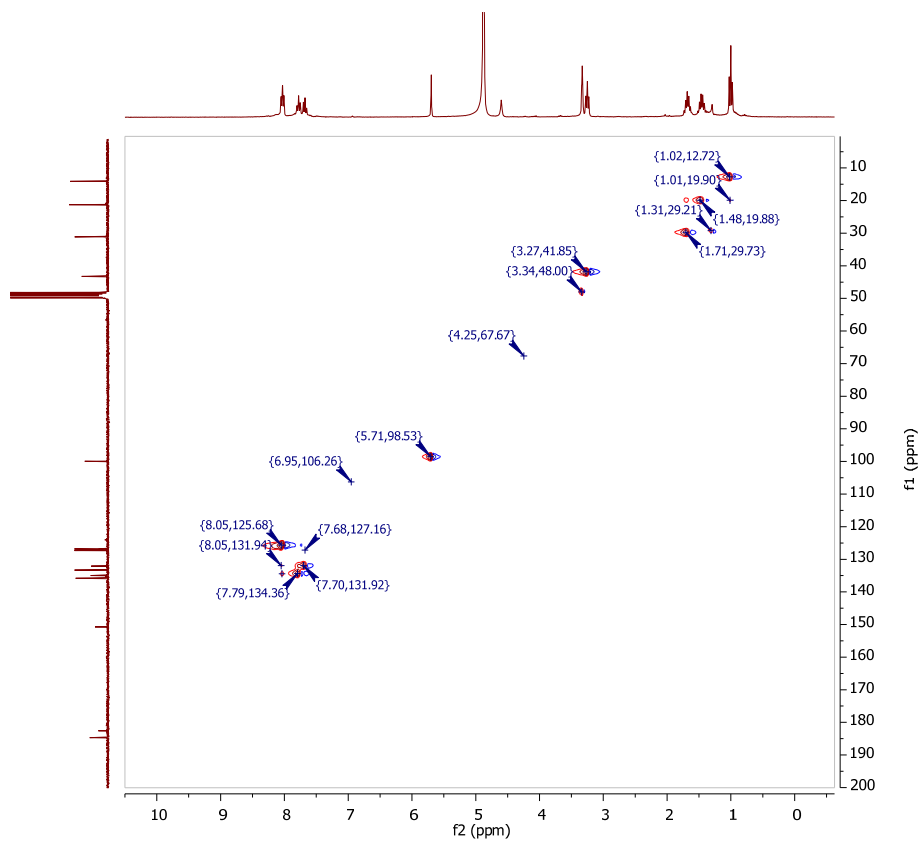


Figure S32. HSQC-NMR spectrum of compound **3e** in MeOD-*d*₄

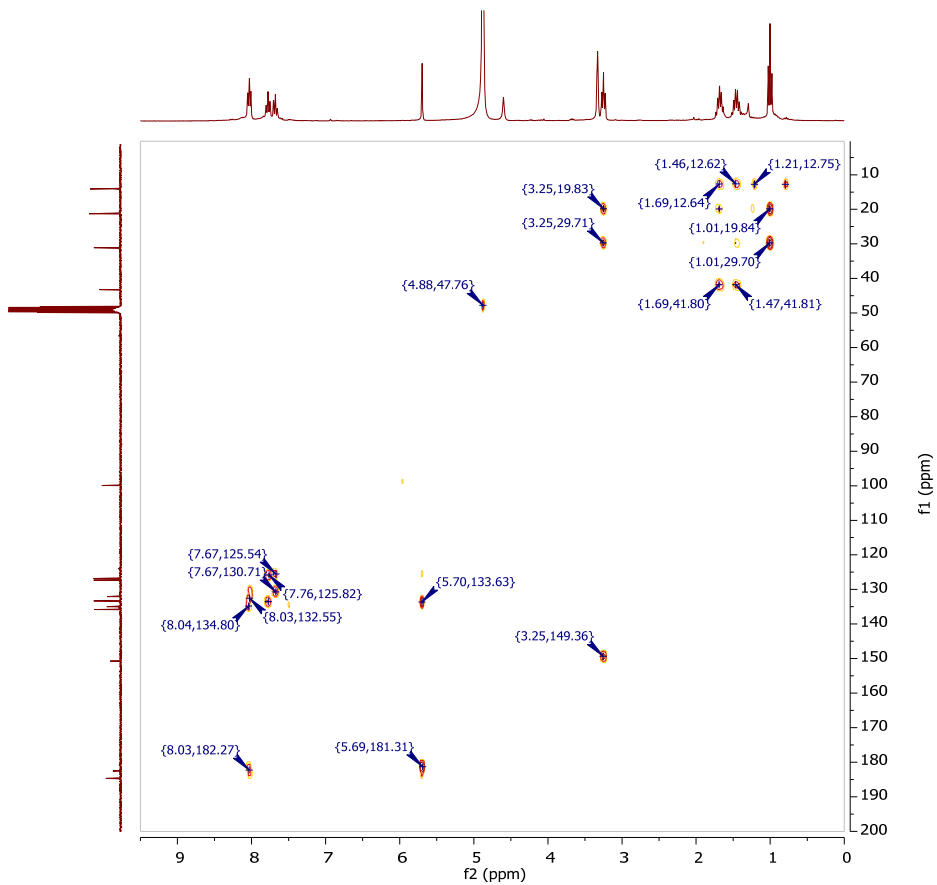


Figure S33. HMBC-NMR spectrum of compound **3e** in MeOD-*d*₄

Compound 3f:

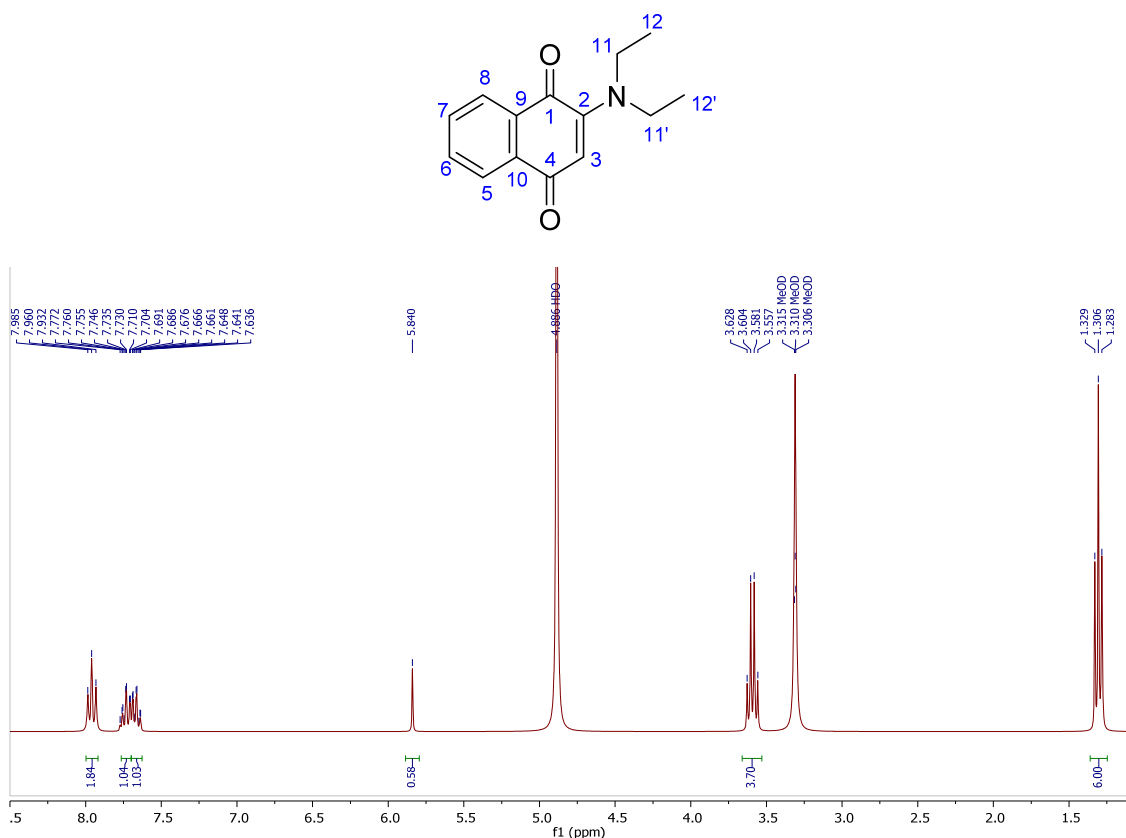


Figure S34. ¹H-NMR spectrum of compound 3f in MeOD-d₄

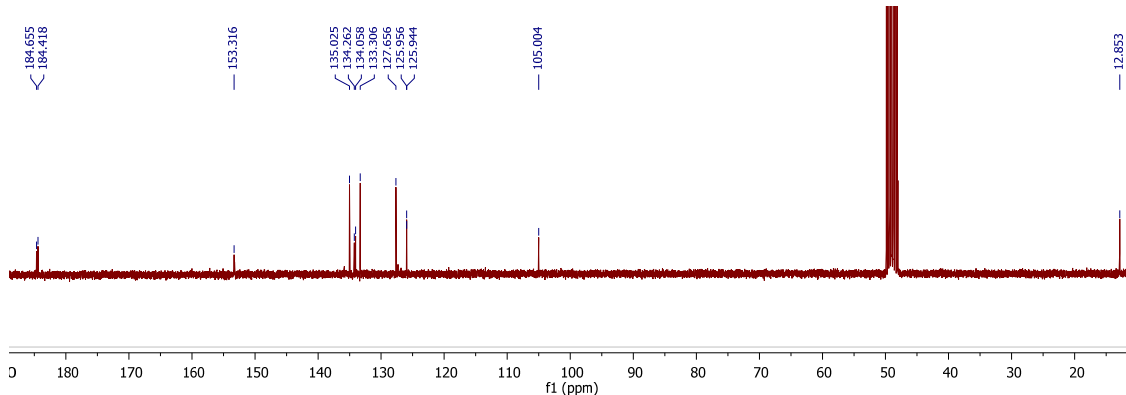


Figure S35. ¹³C-NMR spectrum of compound 3f in MeOD-d₄

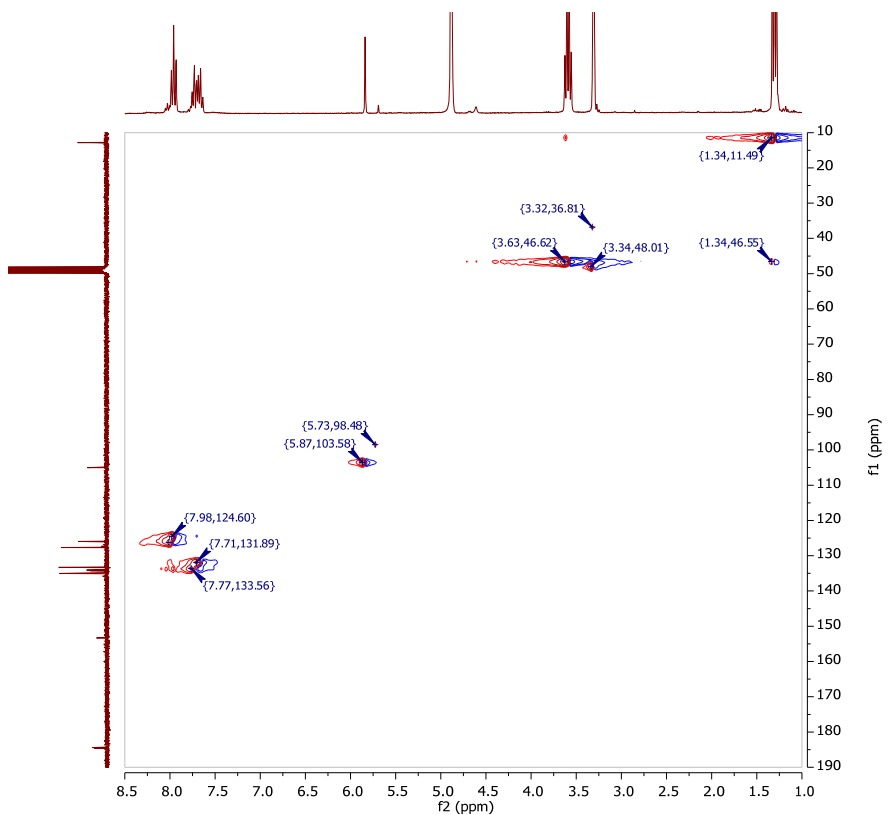


Figure S36. HSQC-NMR spectrum of compound **3f** in MeOD-*d*₄

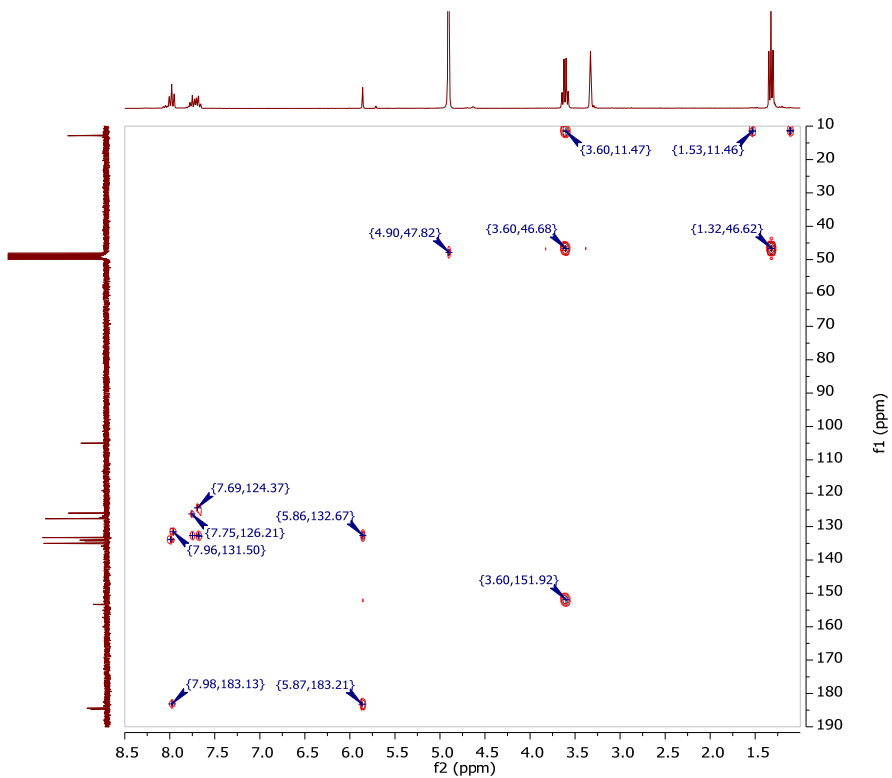


Figure S37. HMBC-NMR spectrum of compound **3f** in MeOD-*d*₄

Compound 4e:

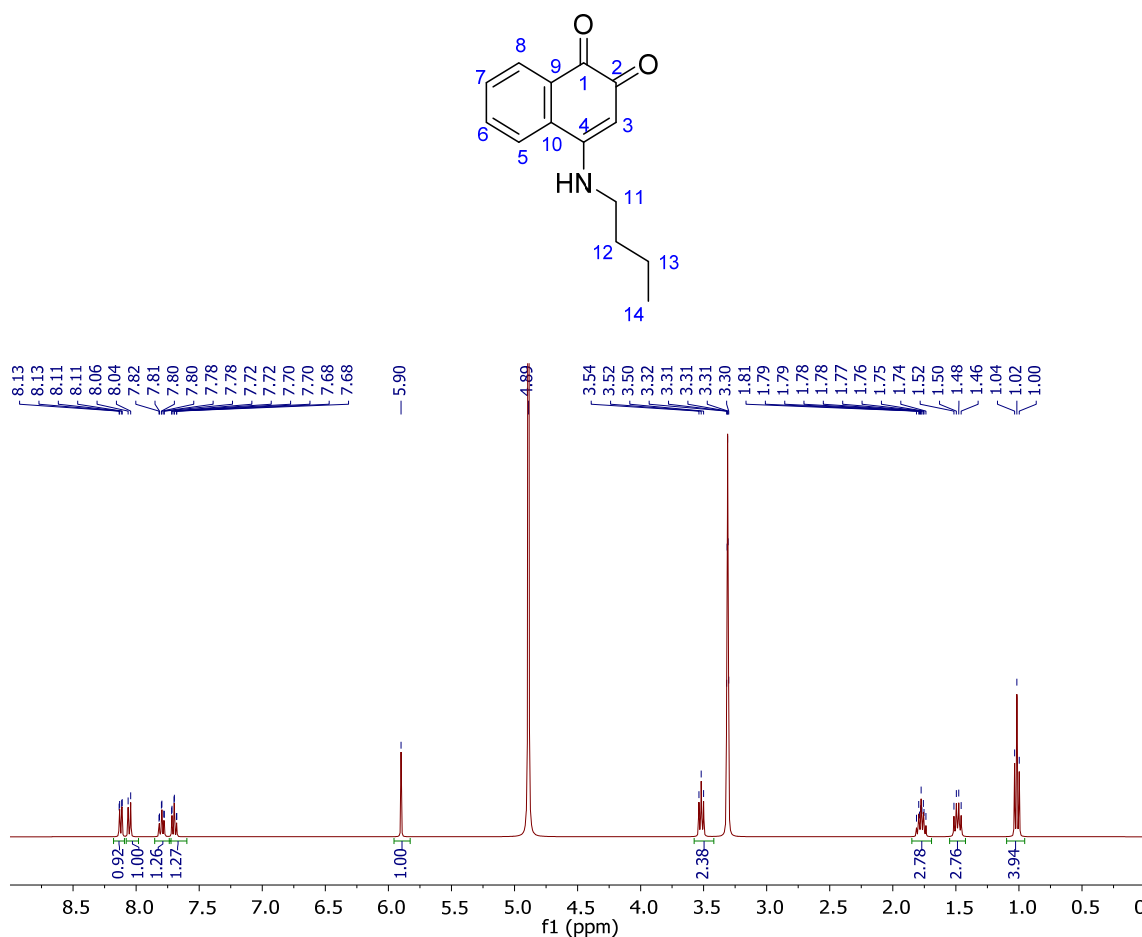


Figure S38. ¹H-NMR spectrum of compound 4e in MeOD-*d*₄

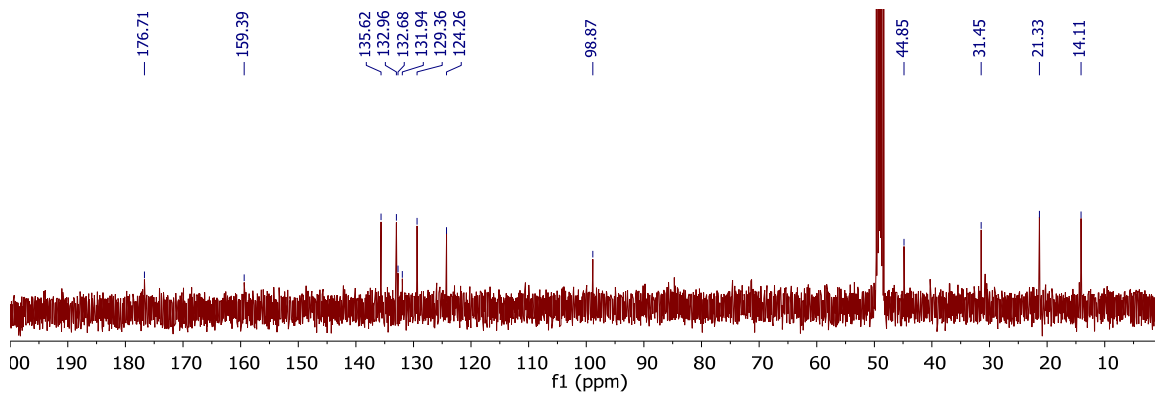


Figure S39. ¹³C-NMR spectrum of compound 4e in MeOD-*d*₄

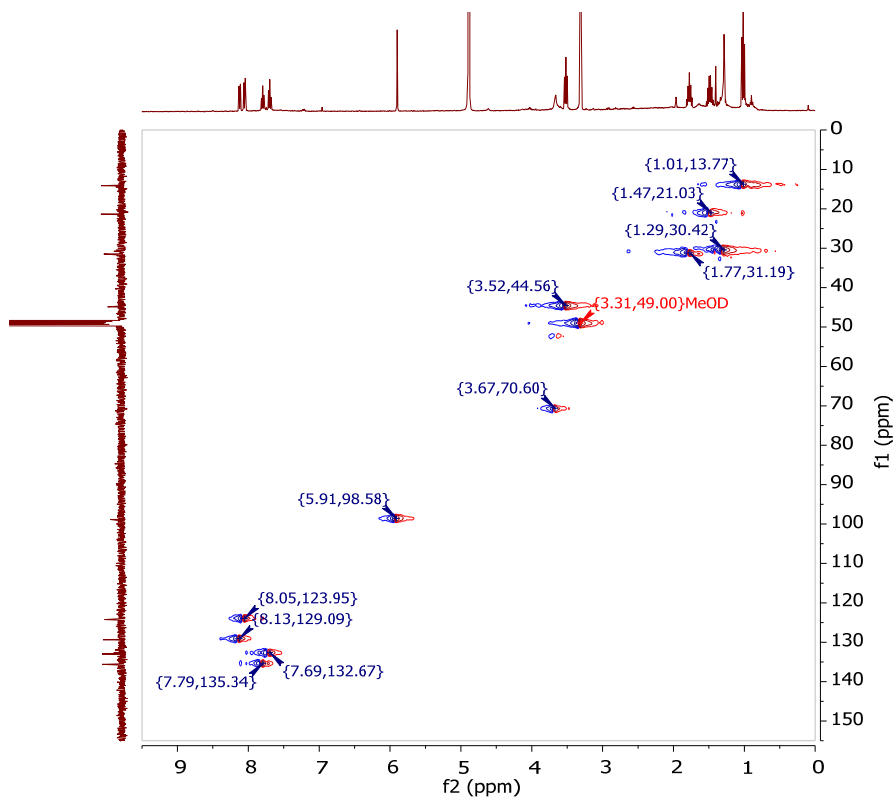


Figure S40. HSQC-NMR spectrum of compound **4e** in $\text{MeOD}-d_4$

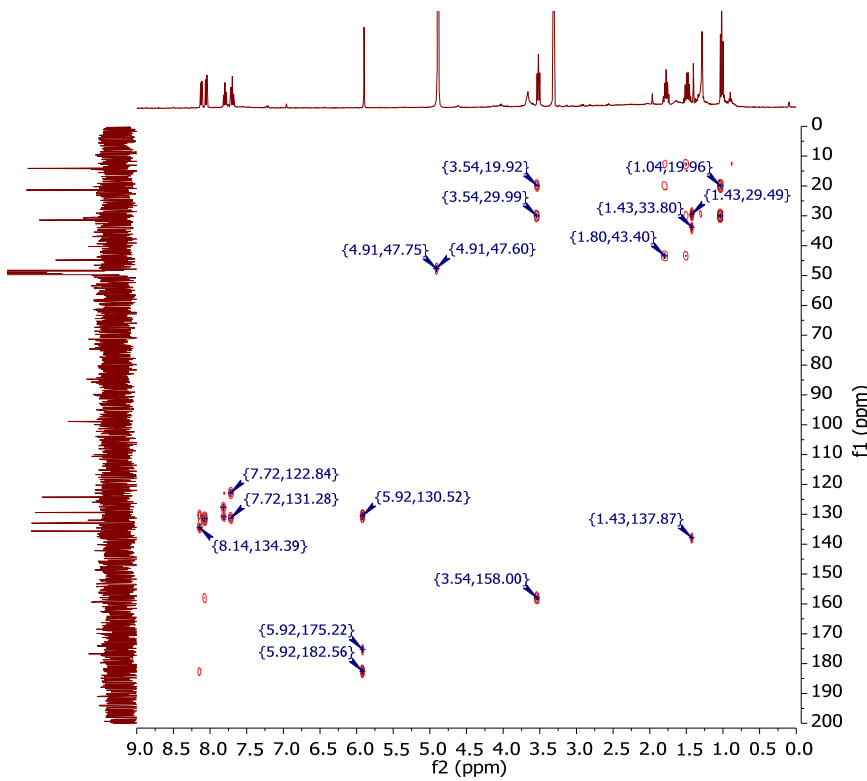


Figure S41. HMBC-NMR spectrum of compound **4e** in $\text{MeOD}-d_4$

Compound 4f:

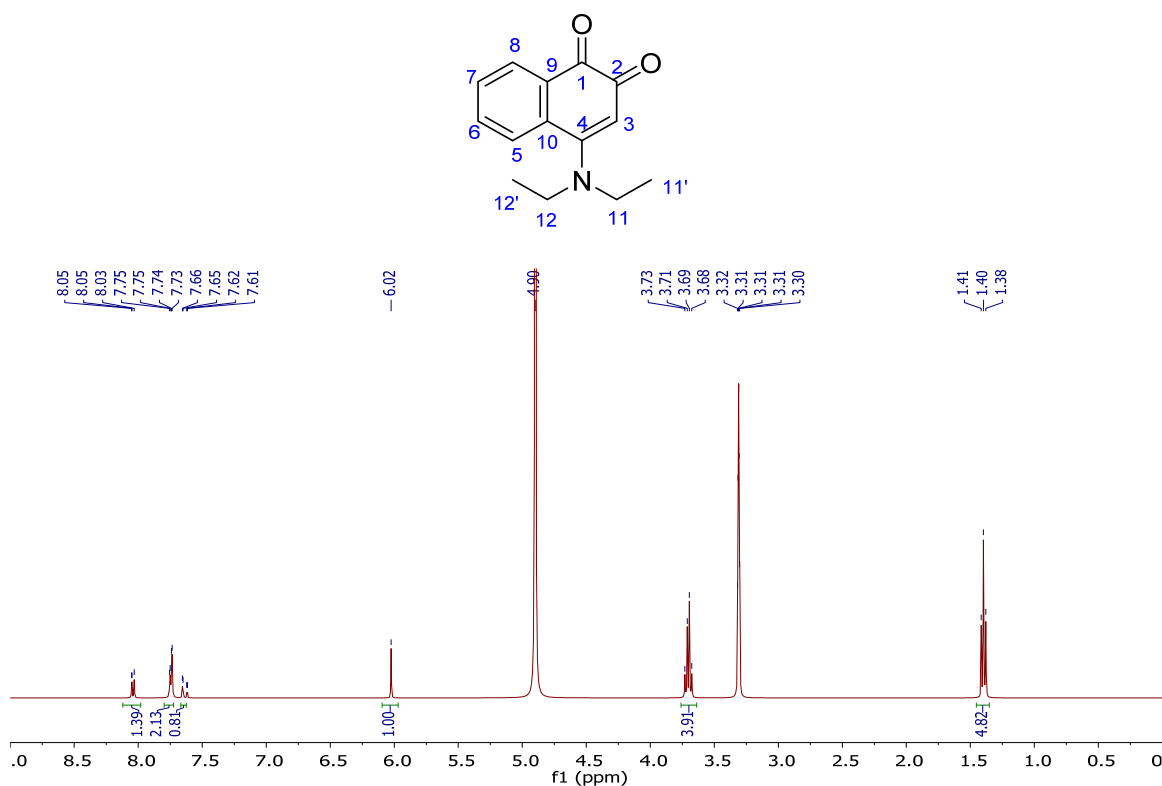


Figure 1S42. ^1H -NMR spectrum of compound **4e** in $\text{MeOD}-d_4$

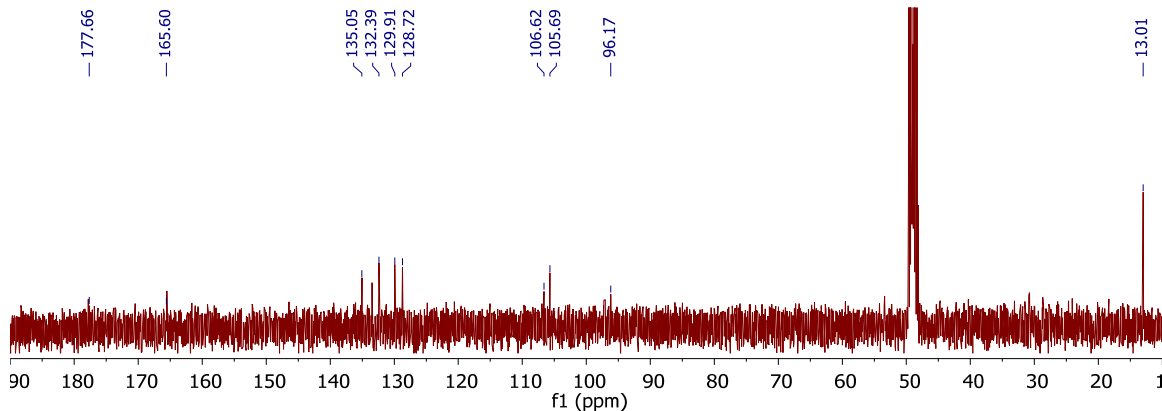


Figure S43. ^{13}C -NMR spectrum of compound **4e** in $\text{MeOD}-d_4$

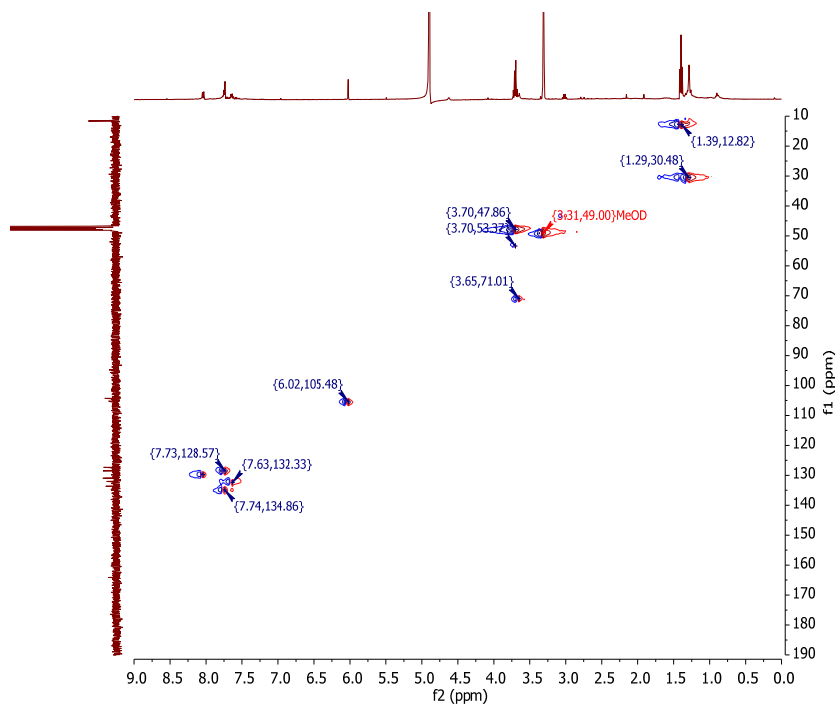


Figure S44. HSQC-NMR spectrum of compound **4e** in $\text{MeOD}-d_4$

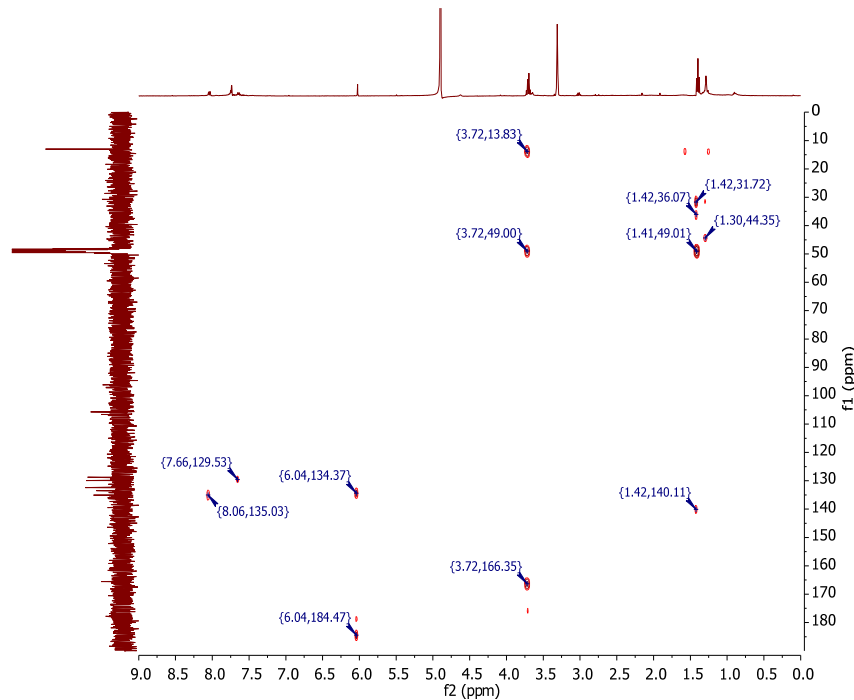


Figure S45. HMBC-NMR spectrum of compound **4e** in $\text{MeOD}-d_4$

Compound 4h:

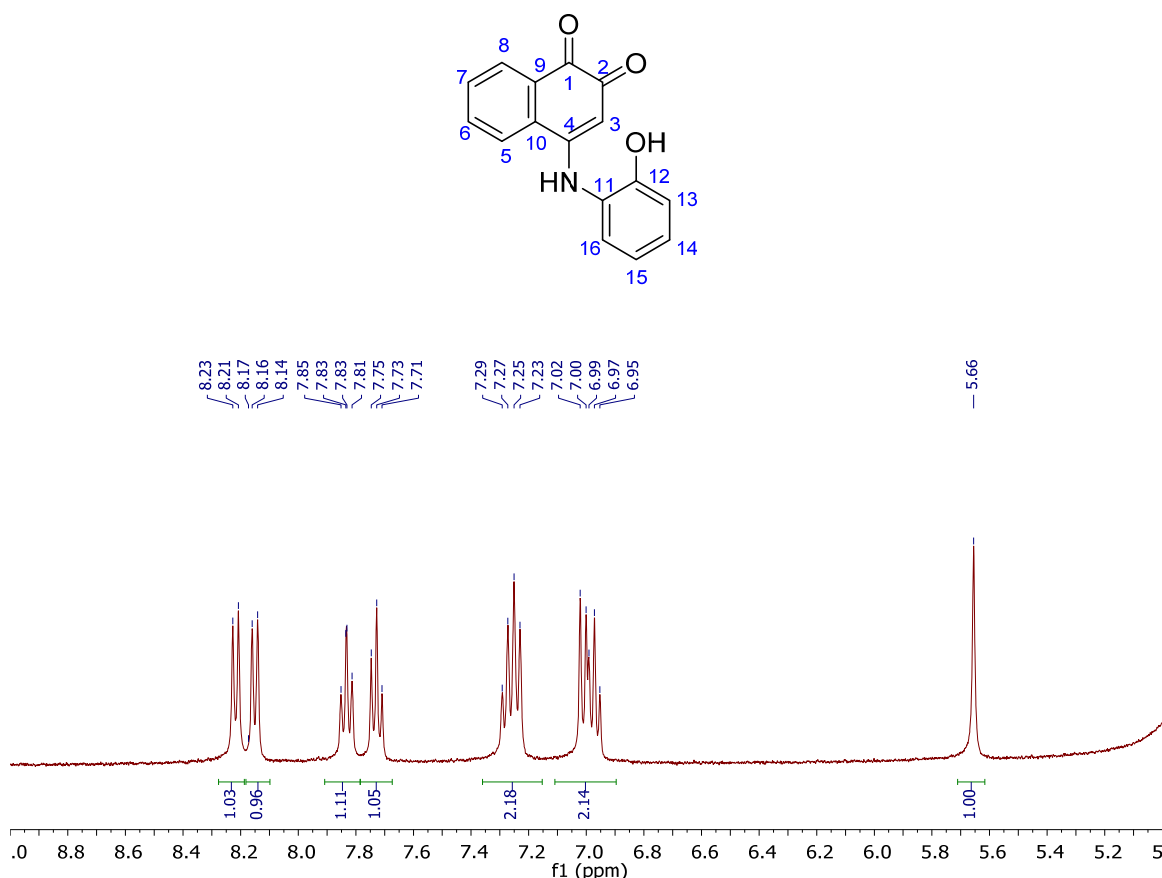


Figure S46. ¹H-NMR spectrum of compound **4h** in MeOD-d₄

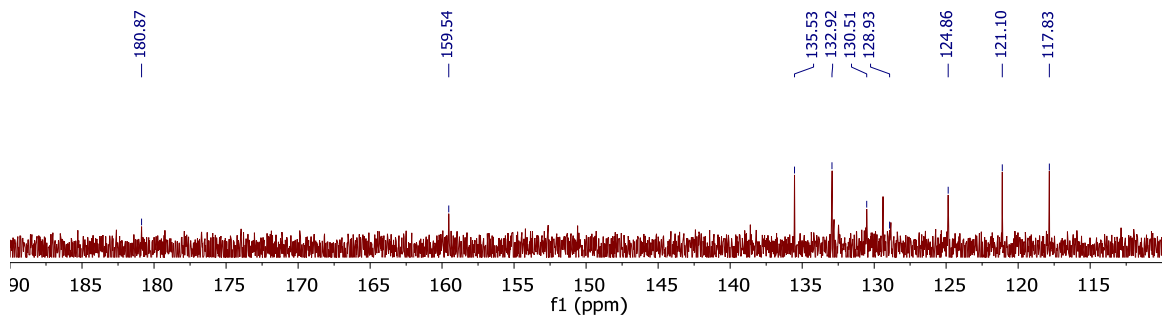


Figure S47. ¹³C-NMR spectrum of compound **4h** in MeOD-d₄

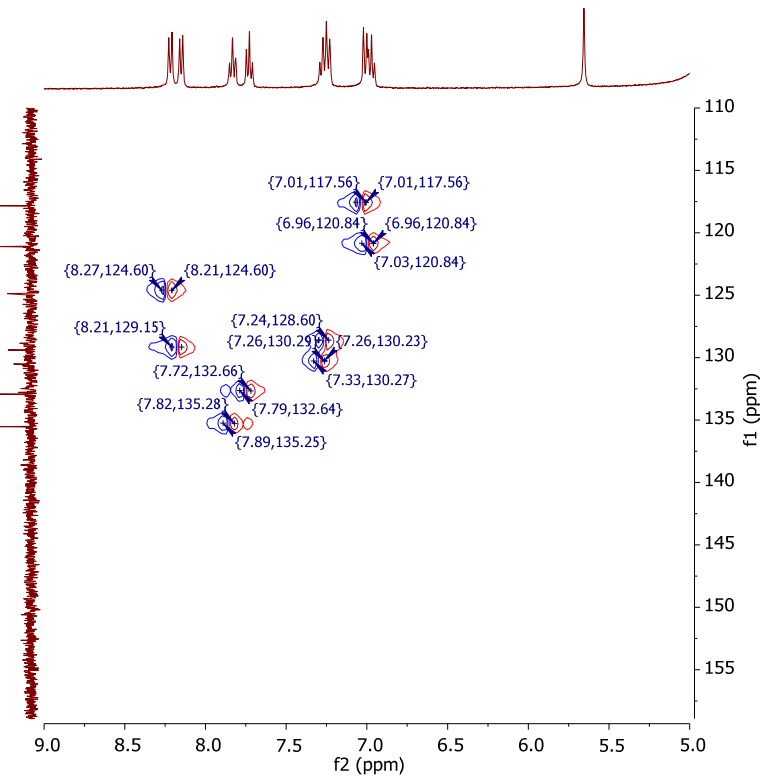


Figure S48. HSQC-NMR spectrum of compound **4h** in MeOD-*d*₄

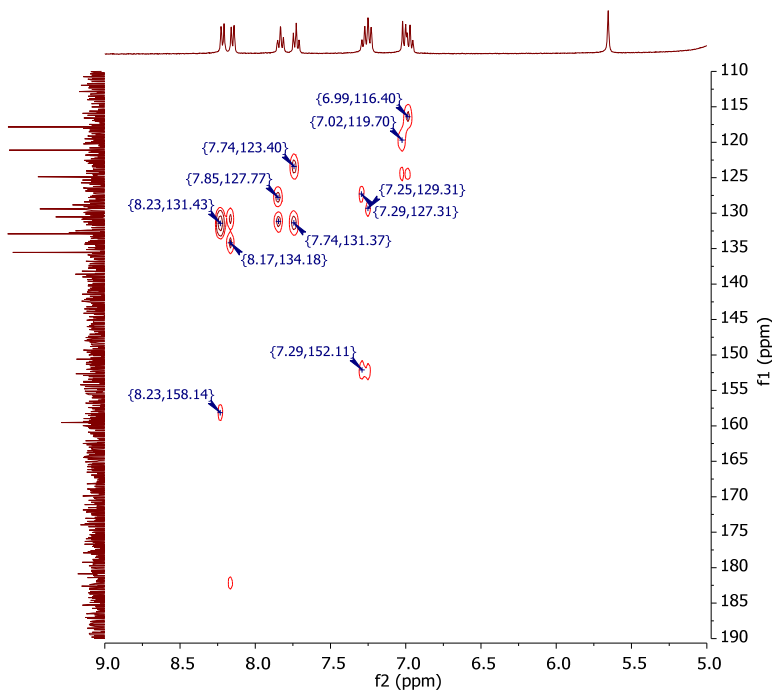


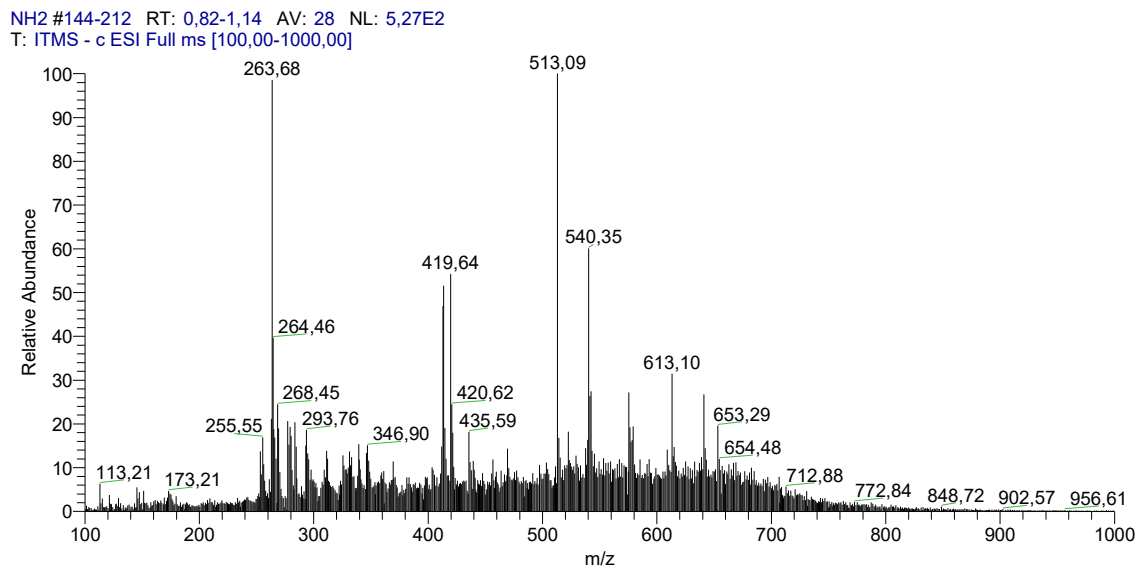
Figure S49. HMBC-NMR spectrum of compound **4h** in MeOD-*d*₄

8. ESI/MS spectra

ESI/MS spectra of compound **3a** ($C_{16}H_{12}N_2O_2$) MW= 264.3 g/mol

Negative mode $m/z = 263$ [$M-H^-$]; Positive mode $m/z = 265$ [$M+H^+$];

A)



B)

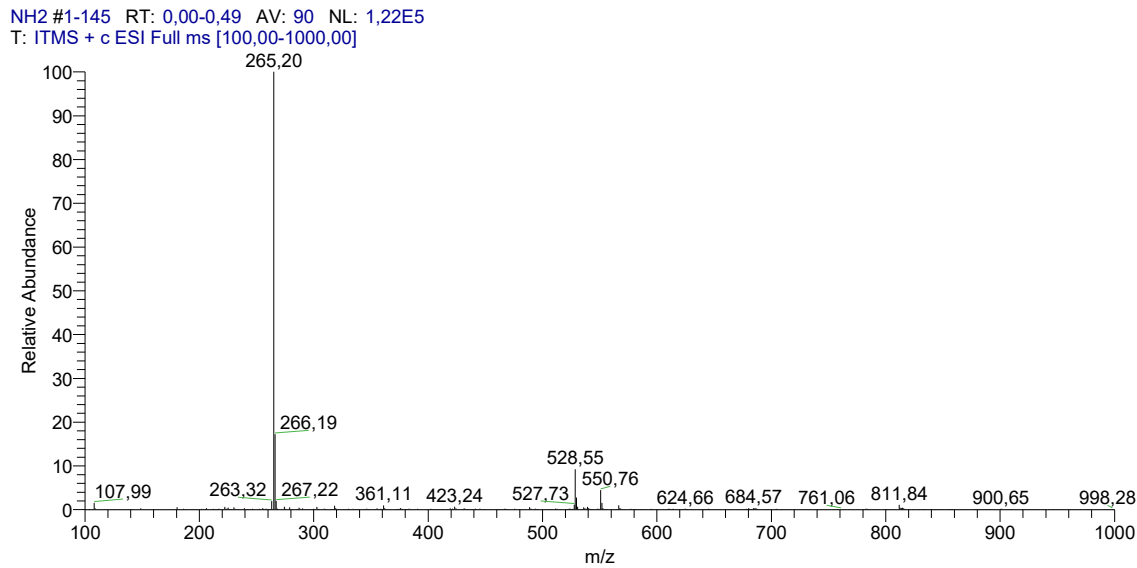


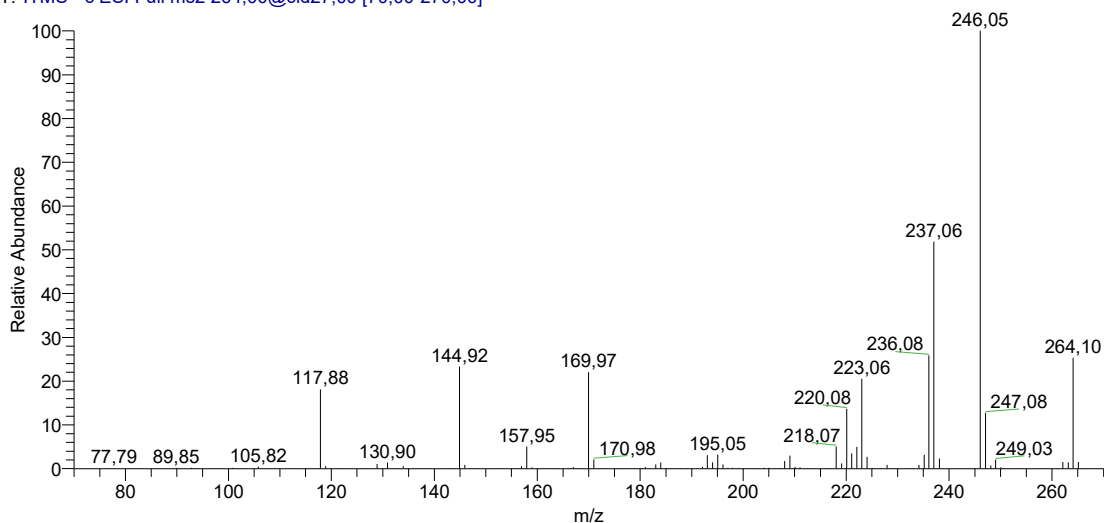
Figure S50. A) ESI(-)/MS spectrum of compound **3a**; C) ESI(+)/MS spectrum of compound **3a**.

ESI/MS spectra of compound **3b** ($C_{16}H_{11}NO_3$) MW= 265.3 g/mol

Negative mode m/z = 264 [$M-H^-$]; Positive mode m/z = 266 [$M+H^+$];

A)

OH #453-563 RT: 2,24-3,18 AV: 111 NL: 2,79E3
T: ITMS - c ESI Full ms2 264,00 [cid27,00 [70,00-270,00]



B)

OH #137-329 RT: 0,60-1,64 AV: 193 NL: 7,08E3
T: ITMS + c ESI Full ms2 266,00 [cid27,00 [70,00-271,00]

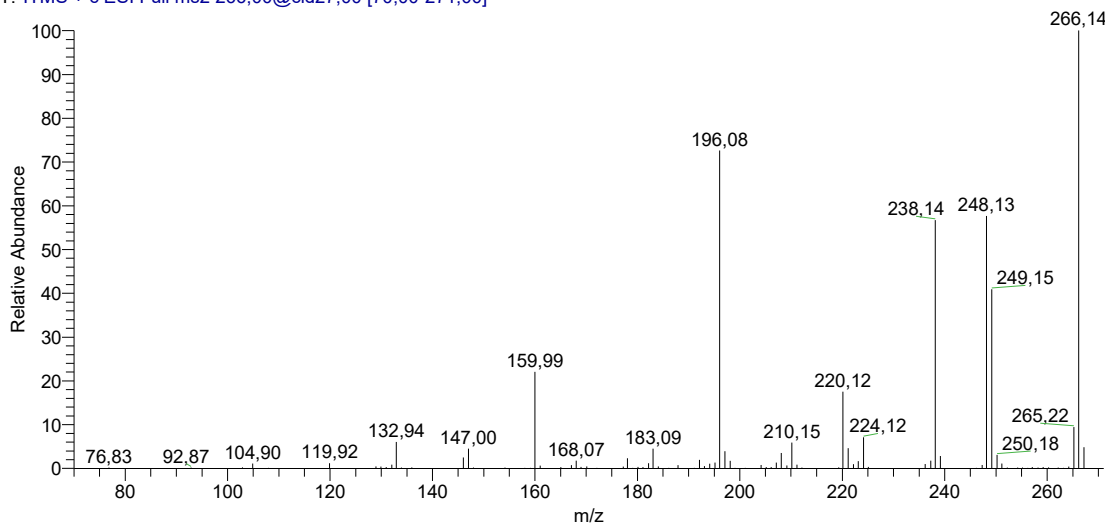


Figure S51. A) ESI(-)/MS spectrum of compound **3b**, B) ESI(+)/MS spectrum of compound **3b**.

ESI/MS spectra of compound **3c** ($C_{16}H_{11}NO_3$) MW= 279.1 g/mol

Positive mode $m/z = 280 [M+H]^+$;

OCH3 #1-84 RT: 0,00-0,38 AV: 84 NL: 1,40E4
T: ITMS + c ESI Full ms [135,00-700,00]

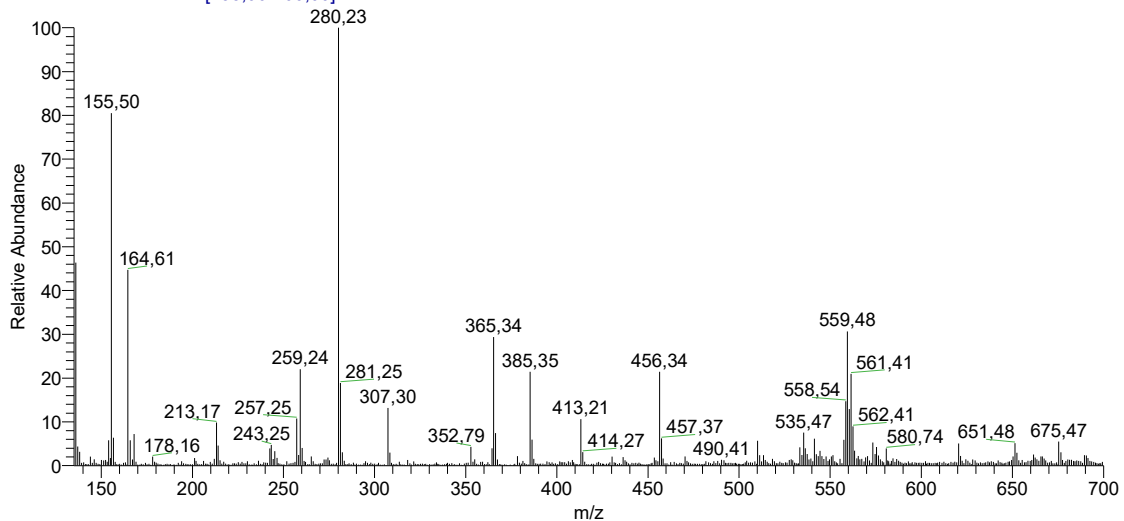


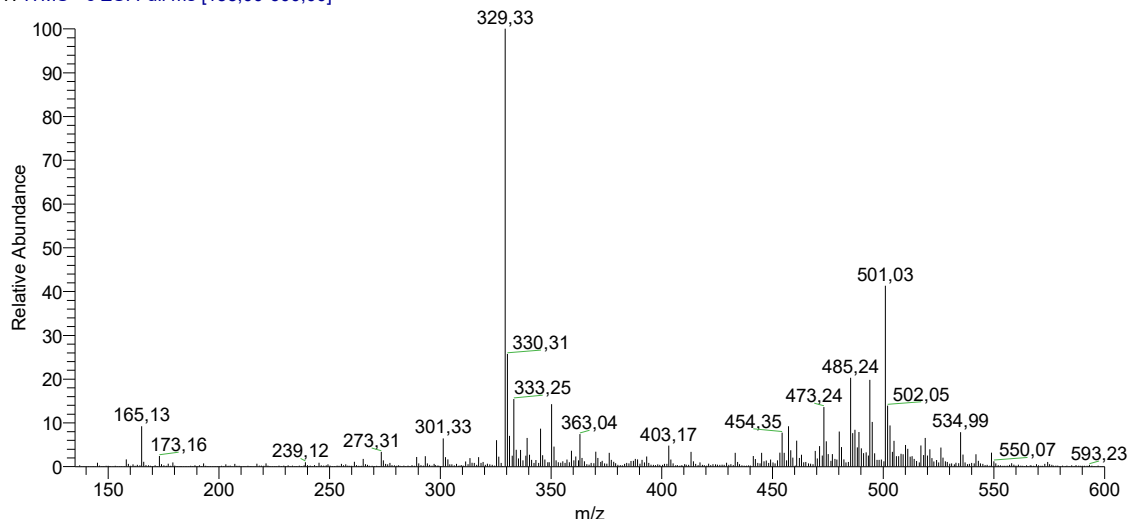
Figure S52. ESI(+)/MS spectrum of compound **3c**.

ESI/MS spectra of compound **3d** ($C_{16}H_{11}NO_3$) MW= 274.1 g/mol

Negative mode m/z = 273 [$M-H^-$]; Positive mode m/z = 275 [$M+H^+$];

A)

CN #20-182 RT: 0,08-0,75 AV: 163 NL: 6,11E4
T: ITMS - c ESI Full ms [135,00-600,00]



B)

CN #363-458 RT: 1,54-2,67 AV: 96 NL: 3,38E1
T: ITMS + c ESI Full ms2 275,00@cid27,00 [75,00-280,00]

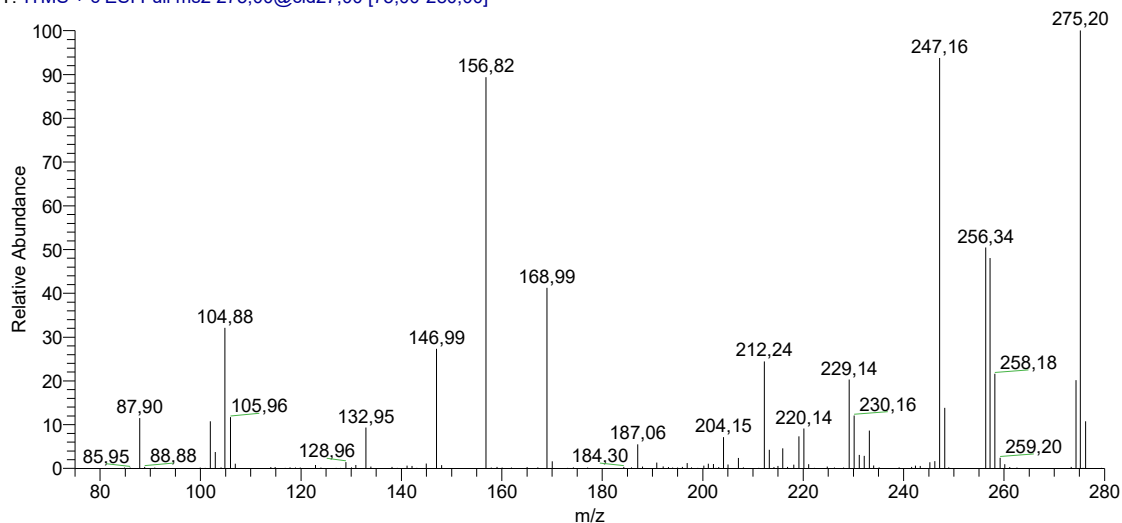
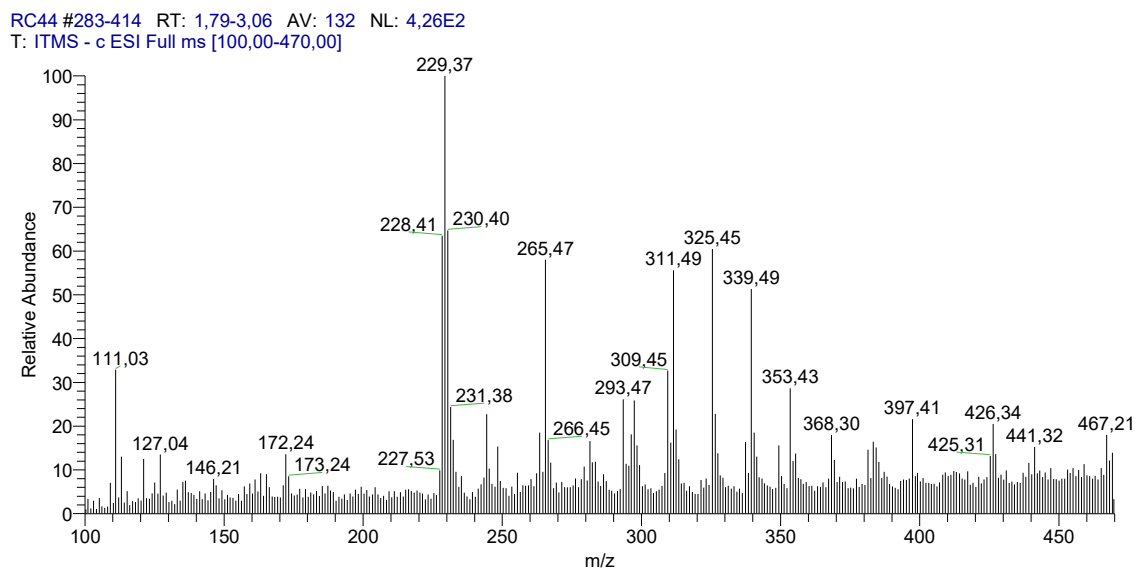


Figure S53. A) ESI(-)/MS spectrum of compound **3d**, B) ESI(+)/MS spectrum of **3d**.

ESI/MS spectra of compound **3e** ($C_{14}H_{15}NO_2$) MW= 229.1 g/mol

Negative mode m/z = 228 [$M-H^-$]; Positive mode m/z = 230 [$M+H^+$];

A)



B)

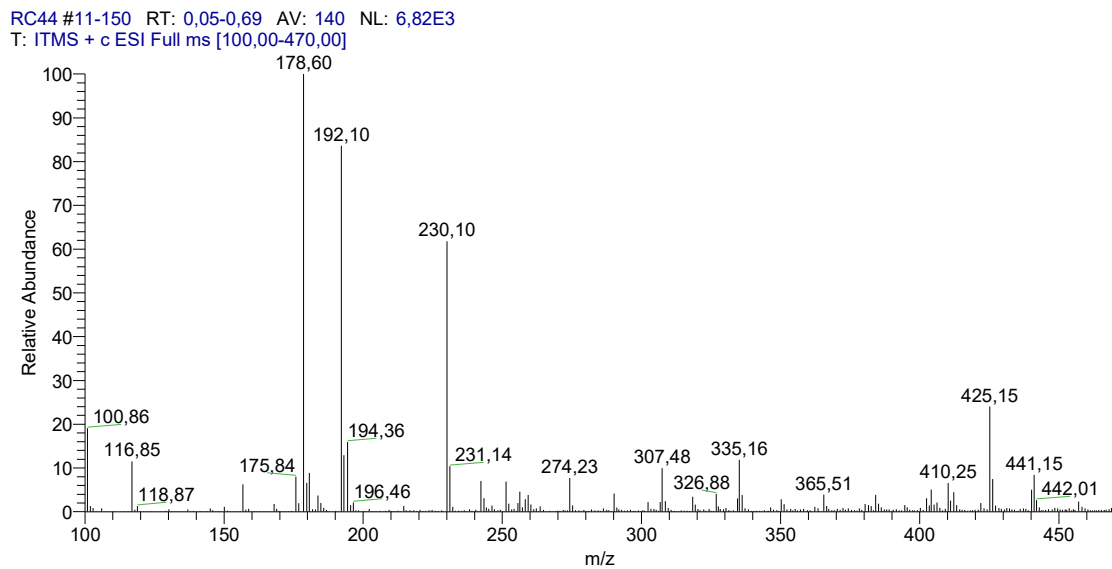


Figure S54. A) ESI(-)/MS spectrum of compound **3e**, B) ESI(+)/MS spectrum of compound **3e**.

ESI/MS spectra of compound **3f** ($C_{14}H_{15}NO_2$) MW= 229.11 g/mol

Positive mode $m/z = 230 [M+H]^+$;

RC49-purificado #13-184 RT: 0,06-0,86 AV: 172 NL: 9,58E3
T: ITMS + c ESI Full ms [100,00-600,00]

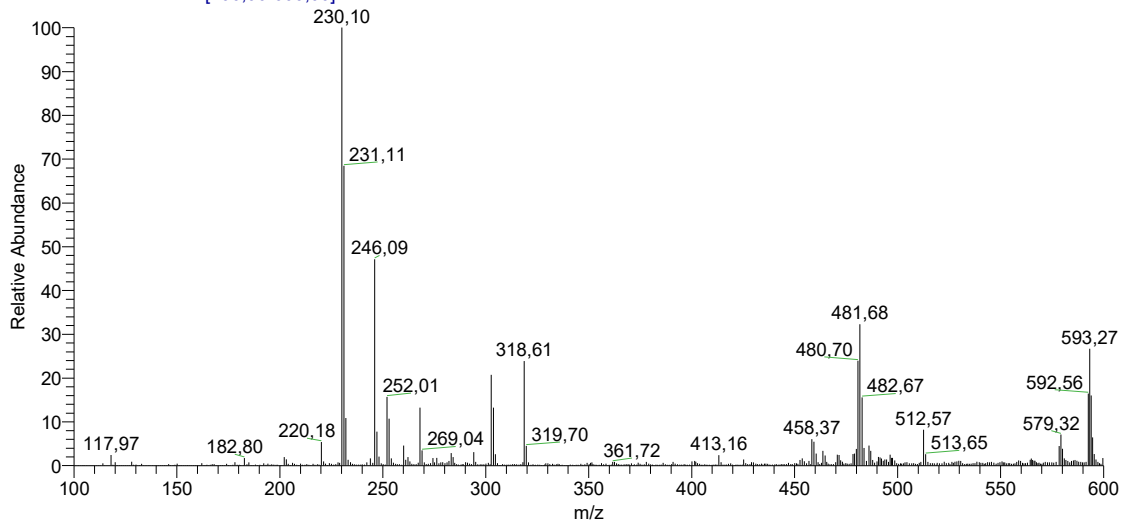
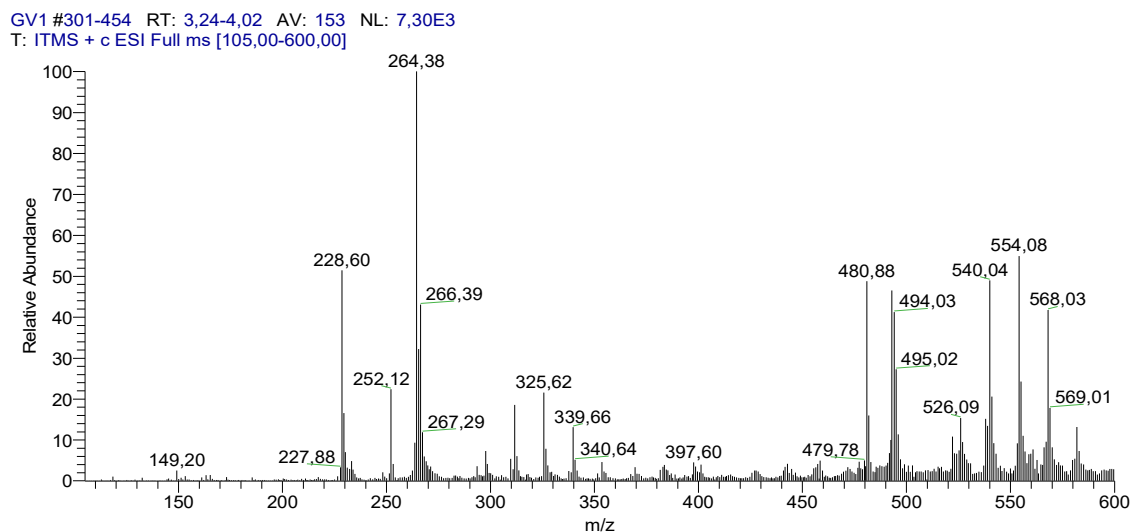


Figure S55. ESI(+)/MS spectrum of compound **3f**.

ESI/MS spectra of compound **4e** ($C_{14}H_{15}NO_2$) MW= 229.1 g/mol

Negative mode m/z = 228 [$M-H^-$]; Positive mode m/z = 230 [$M+H^+$];

A)



B)

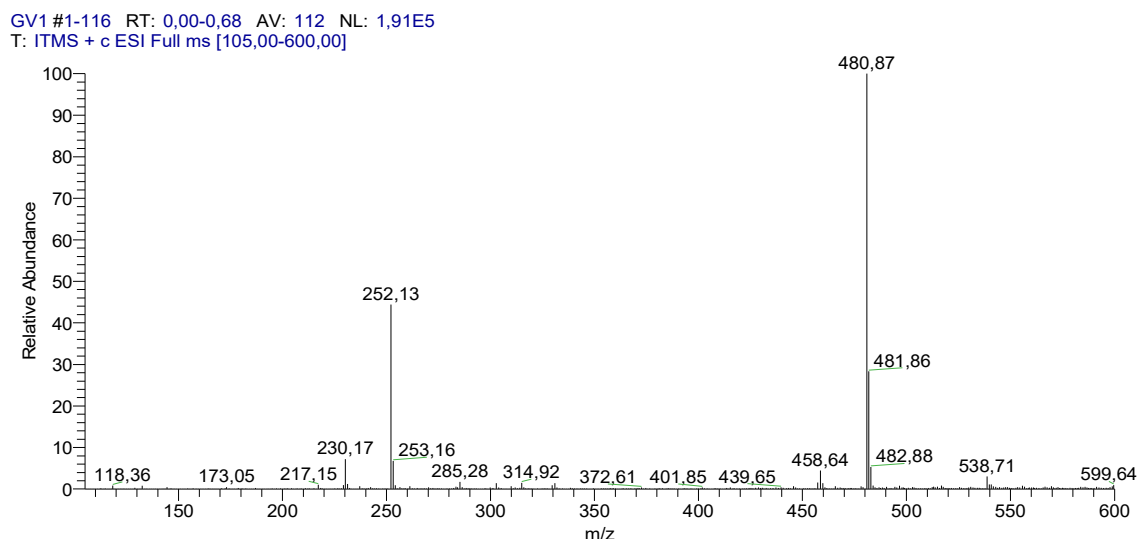


Figure S56. A) ESI(-)/MS spectrum of compound **4e**, B) ESI(+)/MS spectrum of compound **4e**.

ESI/MS spectra of compound **4f** ($C_{14}H_{15}NO_2$) MW= 229.11 g/mol

Positive mode $m/z = 230 [M+H]^+$;

GV3 #1-94 RT: 0,00-0,53 AV: 87 NL: 6,00E4
T: ITMS + c ESI Full ms [105,00-600,00]

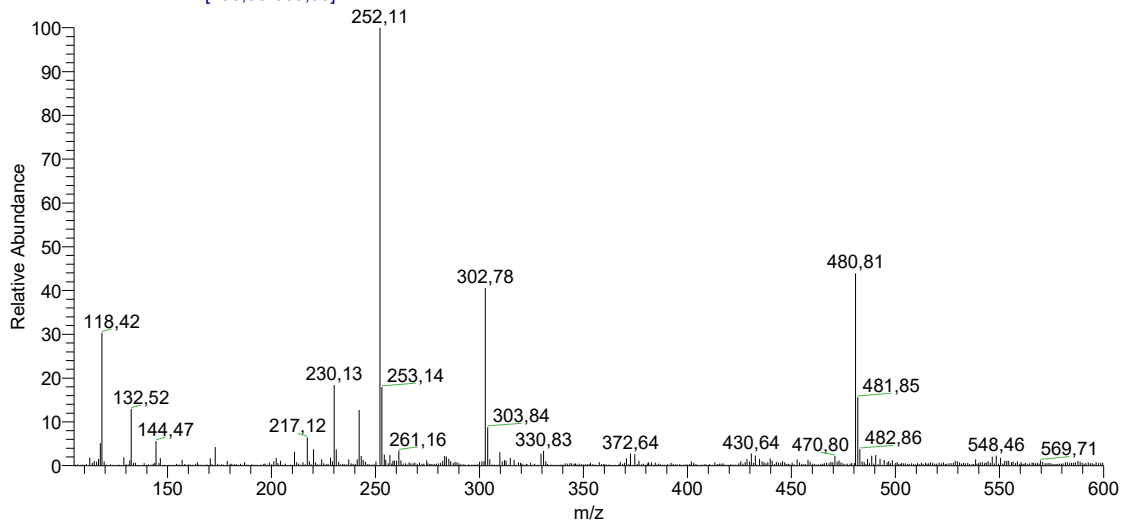


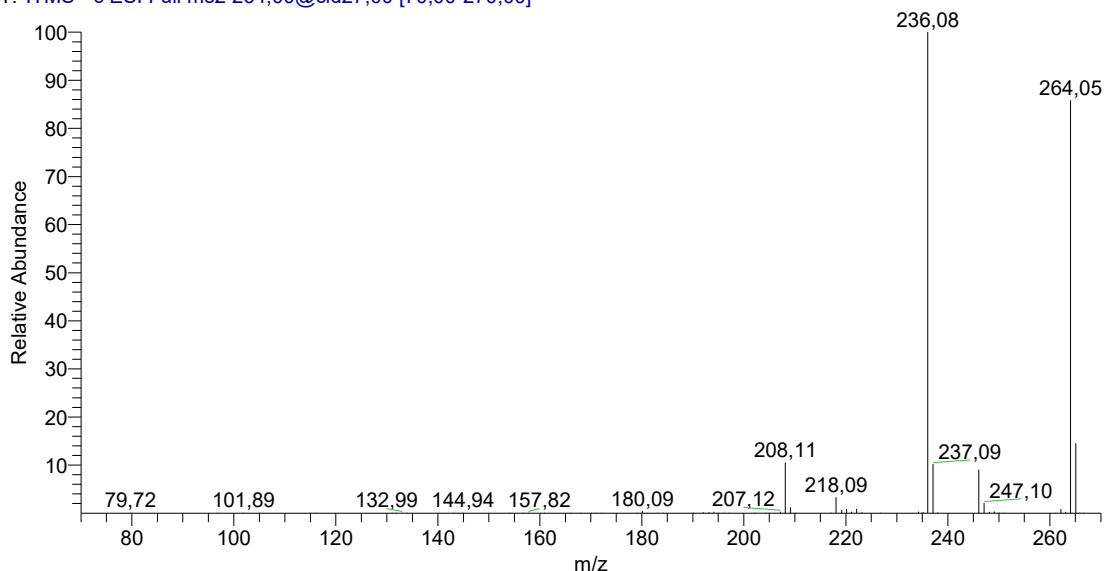
Figure S57. ESI(+)/MS spectrum of compound **4f**.

ESI/MS spectra of compound **4h** ($C_{16}H_{11}NO_3$) MW= 265.3 g/mol

Negative mode m/z = 264 [$M-H^-$]; Positive mode m/z = 266 [$M+H^+$];

A)

OH #308-377 RT: 2,14-2,48 AV: 28 NL: 1,58E3
T: ITMS - c ESI Full ms2 264,00@cid27,00 [70,00-270,00]



B)

OH #1-102 RT: 0,00-0,52 AV: 102 NL: 1,26E4
T: ITMS + c ESI Full ms [100,00-650,00]

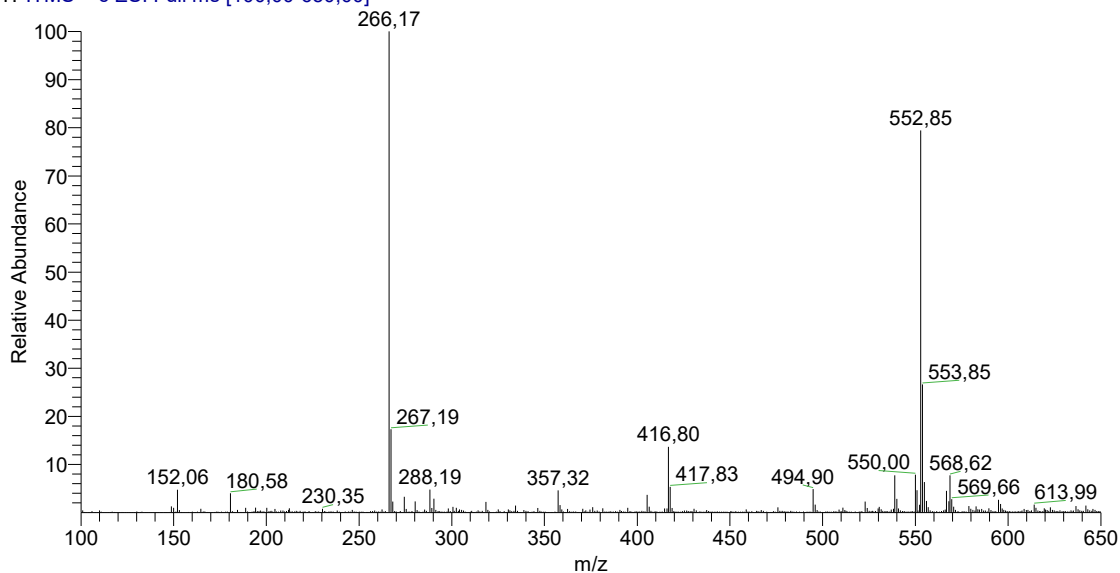


Figure S58. A) ESI(-)/MS spectrum of compound **4h**, B)) ESI(+)/MS spectrum of compound **4h**.

9. HRESI/TOFMS spectra

Acquisition Parameter

Source Type	ESI	Ion Polarity	Positive	Set Nebulizer	2.8 Bar
Focus	Active	Set Capillary	4500 V	Set Dry Heater	200 °C
Scan Begin	100 m/z	Set End Plate Offset	-500 V	Set Dry Gas	8.0 l/min
Scan End	1000 m/z	Set Charging Voltage	2000 V	Set Divert Valve	Waste
		Set Corona	0 nA	Set APCI Heater	0 °C

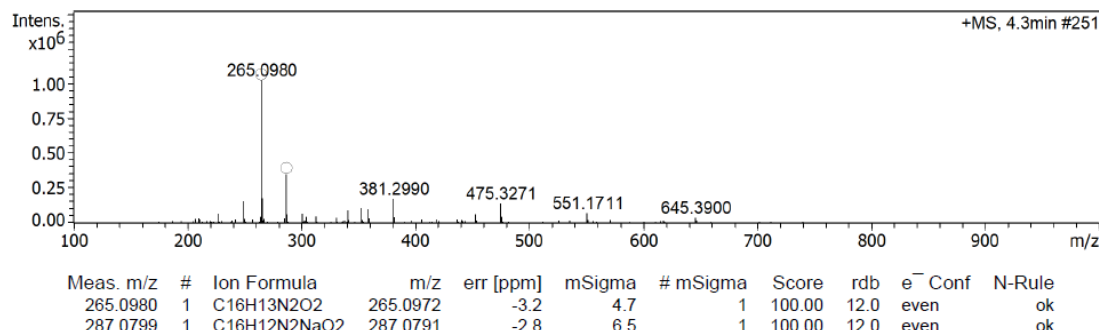


Figure S59. HR ESI(+)/MS spectrum of compound **3a**.

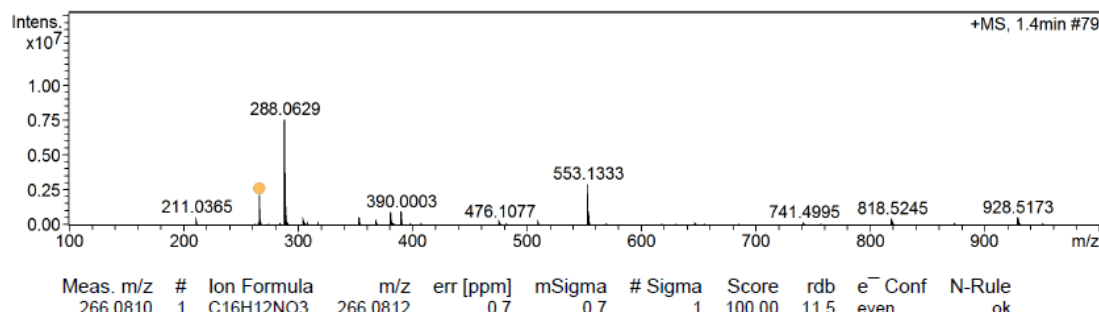


Figure S60. HR ESI(+)/MS spectrum of compound **3b**.

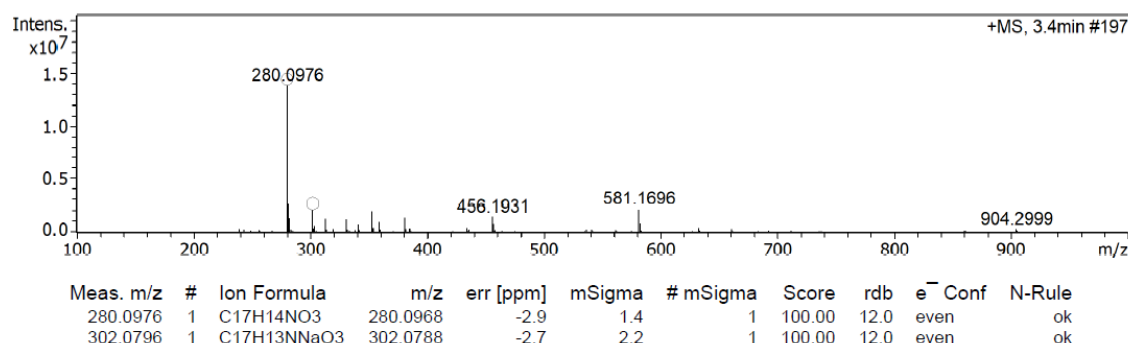


Figure S61. HR ESI(+)/MS spectrum of compound **3c**.

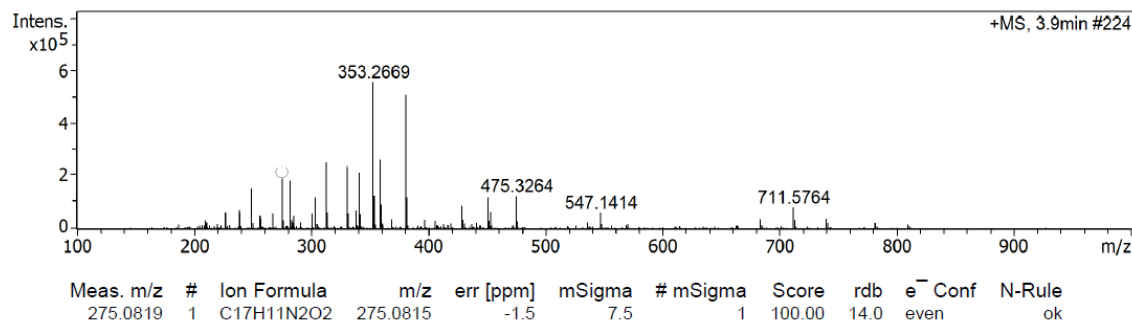


Figure S62. HR ESI(+) /MS spectrum of compound **3d**.

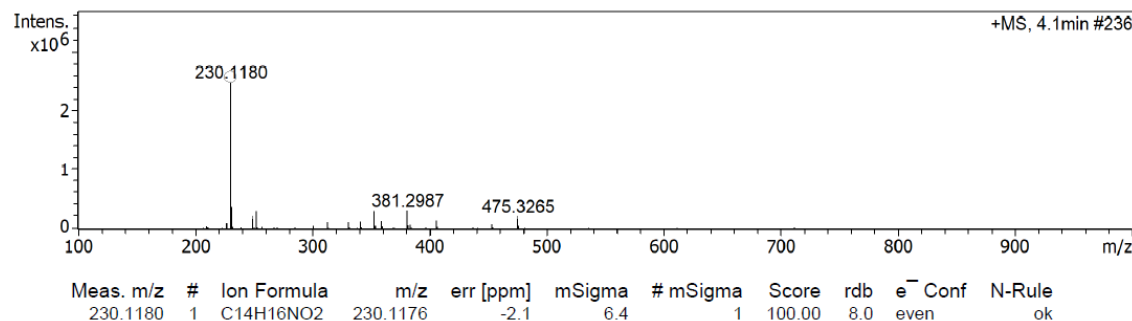


Figure S63. HR ESI(+) /MS spectrum of compound **3e**

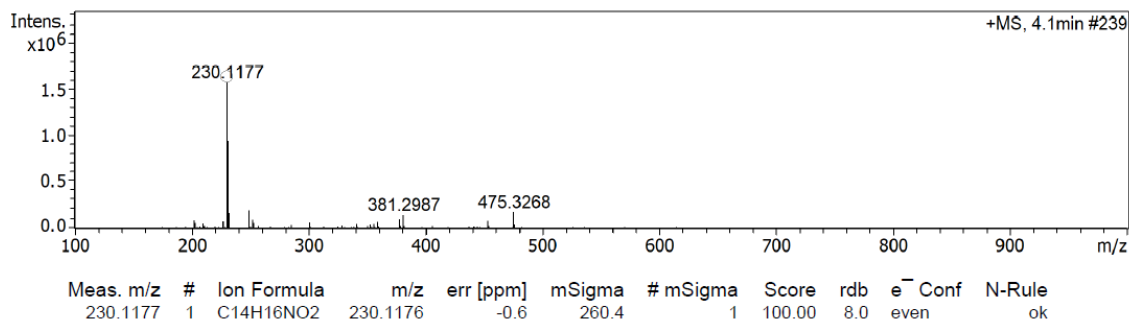


Figure S64. HR ESI(+) /MS spectrum of compound **3f**.

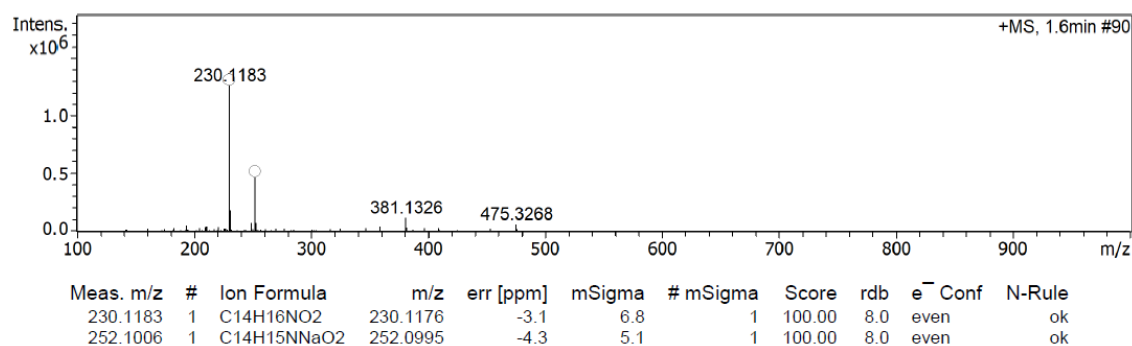


Figure S65. HR ESI(+)MS spectrum of compound **4e**

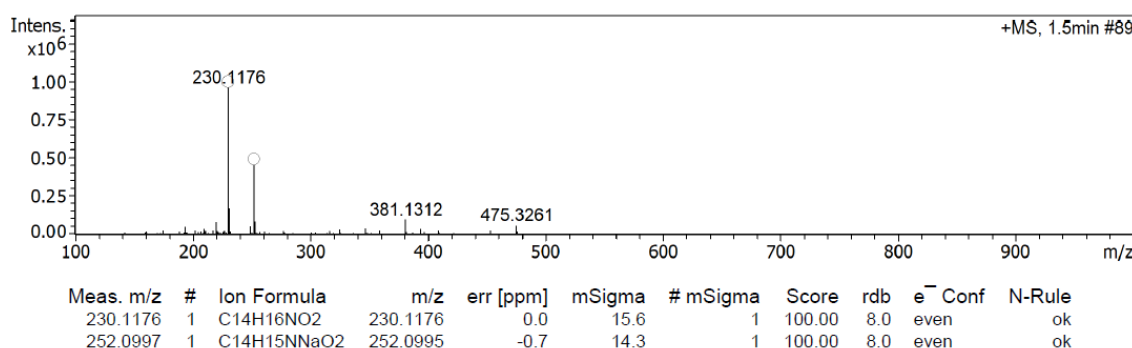


Figure S66. HR ESI(+)MS spectrum of compound **4f**.